A STUDY OF HYDROXYL MASERS IN THE CIRCUMSTELLAR ENVELOPES OF LONG PERIOD VARIABLE STARS

Thesis by

Menachem Cimerman

In Partial Fulfillment of the Requirements

for the Degree of

Doctor of Philosophy

California Institute of Technology

Pasadena, California

1980

(Submitted May 9, 1979)

ACKNOWLEDGEMENTS

It all began when Tel Aviv University was planning to get into radio astronomy (circa 1973). Asher Gotessman, then the head of the Physics and Astronomy Department and Yuval Ne'eman, then the president of the University encouraged me to get involved, and this brought me to Caltech. I am grateful to these two and to my alma mater for the encouragement and support.

My first adviser at Caltech, Marshall Cohen, deserves many thanks for the help and guidance he has given me, even though I have not worked in VLBI. His moral support sustained me through more than one crisis.

Peter Wannier took over as my adviser during the last phase of my graduate work. He is appreciated for his encouragement of my theoretical efforts. Peter deserves any credit for my ability to write papers; he practically taught me how to do it.

Peter Goldreich was the moving force behind this work. The observing program was instigated by him, and he encouraged my theoretical endeavor. Most of all he is acknowledged for making available to me his insight and wit.

Nick Scoville introduced me to the radio observatory and helped me get started with the observing program. Later on he became a collaborator in the theoretical work.

The intricacies of the interferometer were revealed to me by Glenn Berge, Dave Rogstad, and George Seielstad.

The observations were made possible by the concerted work of the Owens Valley Radio Observatory personnel directed by Al Moffet and previously by Gordon Stanley. Engineering support was provided by Wayne Hammond, Harry Hardebeck, Bob Shattuck, and Chuck Spencer. Carol Walton and Jill Bechtold assisted with the observations. Administrative and secretarial support and much charm were provided by Carol Brown, Faye DeWindt, Alice Fisher, and Jo Ann Pearson.

Many people contributed to my work with advice and stimulation, among them Charles Alcock, Moshe Elitzur, Frank Israel, Jill Knapp, Roger Linfield, Fred Lo, Mark Morris, Mark Reid, Jon Romney, Anneila Sargent, and my office-mate Don Schneider who patiently witnessed my labor pains and the accompanied noise.

Very helpful data were communicated to me by C. Camy-Peyret, J. L. Destombes, J. M. Flaud, J. R. D. Lépine, J. A. Mattei, and J. P. Maillard.

Finally I wish to thank Joanne Clark for typing the manuscript.

My work at Caltech was supported by National Science Foundation grant AST77-00247, tuition scholarships from the Institute, and funds from Tel Aviv University.

ABSTRACT

The 18 cm wavelength maser radiation from long period variable (LPV) stars is emitted by hydroxyl (OH) molecules in the expanding circumstellar envelopes. The four possible transitions within the ground state of the OH molecule are divided into two groups: mainlines at 1665 and 1667 MHz and satellite lines at 1612 and 1720 MHz. Three of these lines are observed in maser radiation from LPV stars: the 1612 MHz line and the mainlines. The observed properties of the 1612 MHz radiation are easier to interpret than those of the mainlines due to the quantum mechanical symmetries of the OH molecule. This investigation tackles the problem of the OH mainline masers, first by radio observations of two LPV sources with unique OH properties, and then by a theoretical analysis.

The U Ori OH masers were monitored following the drastic events in these masers in early 1974. The events consisted of the sudden appearance of strong 1612 MHz radiation, coincident with the disappearance of the 1667 MHz radiation. They are interpreted in light of the monitored evolution of the 1612 MHz radiation, the decline in its output level, and the subsequent re-emergence of a 1667 MHz line. The conclusion is that the events are the outcome of a short-lived disturbance in the stellar photosphere, most likely a shock-wave, which affected the maser through radiative coupling between the photosphere and the OH molecules.

Observations of the OH maser in W Hya are presented, which suggest an explanation of their unique polarization characteristics.

The maser lines may be formed at a distance of $\sim 10^{14}$ cm from the stellar surface in the presence of a magnetic field of $\sim$ 9 milligauss. This magnetic field is coupled to the ionized component of the outflowing circumstellar envelope. In the W Hya case the magnetic field is evident in the strong polarization, Zeeman pattern and differential magnetorotation. However, it may exist unnoticed in other OH sources, and contribute to the pumping mechanism.

The pumping of OH masers in late-type-variables by direct stellar radiation of 2.8μ is studied. Two pumping schemes are suggested based on line coincidences between OH V=0-1 transitions and strong H_2O ν_3 transitions. The water molecules perturb the stellar radiation by absorption, and thus cool the coinciding OH transition. It is demonstrated that this cooling is capable of producing strong OH masers in the circumstellar envelopes of late-type-variables. This model can account for the existence of mainline ($\Delta F=0$) OH masers, which is hard to explain otherwise.

TABLE OF CONTENTS

INTRODUCTION

The 18 cm wavelength maser radiation from long-period-variable (LPV) stars is emitted by hydroxyl (OH) molecules in the expanding circumstellar envelopes.[1] The lambda doubling and hyperfine splitting in the ground state of the OH molecule produce four microwave transitions. Those are divided into two groups: mainlines at 1665 and 1667 MHz and satellite lines at 1612 and 1720 MHz. Three of these lines are observed in maser radiation from LPV stars, namely the 1612 MHz line and the mainlines. The observed properties of the 1612 MHz masers were interpreted by Elitzur, Goldreich, and Scoville (1976). So far no sound model has been suggested for the mainline masers. These are much harder to deal with, since the radiative selection rules of the OH molecule do not discriminate between the lambda doublets.

This study of OH masers in LPV stars emphasizes the problem of the OH mainline masers. The thesis contains three papers written for journal publication (hence some redundancy is present). The first two papers report radio observations of the unique OH sources in U Ori and W Hya. The third paper is a theoretical work in which a model is presented for OH maser pumping by line blockage of stellar radiation at 2.8 microns. This model is capable of explaining the OH mainline masers.

---

[1] The uninitiated reader is referred to review articles by Goldreich (1975), ter Haar and Pelling (1974), and Litvak (1974).

CHAPTER I

THE FLARE IN THE U ORIONIS OH MASER*

*The Astrophysical Journal, 228:L79-L82, 1979 March 1

ABSTRACT

The U Ori OH masers were monitored following the drastic events in these masers in early 1974. The events consisted of the sudden appearance of strong 1612 MHz radiation, coincident with the disappearance of the 1667 MHz radiation. They are interpreted in the light of the monitored evolution of the 1612 MHz radiation, the decline in its output level, and the subsequent reemergence of a 1667 MHz line. The conclusion is that the events are the outcome of a short-lived disturbance in the stellar photosphere, most likely a shock wave, which affected the maser through radiative coupling between the photosphere and the OH molecules.

I. INTRODUCTION

U Ori is a cool, oxygen-rich ([O]/[C]>1) M-type Mira variable. A small excess of infrared radiation in the spectrum of this red giant indicates the existence of a thin dust shell around the star (Wilson et al., 1972). Its circumstellar envelope, which recently experienced a radical change in the 18 cm wavelength OH emission, has been known to emit the following molecular radiation:

1) H_2O maser radiation at 22.235 GHz, detected on 1970 April 30 by Wilson et al. (1972).

2) OH maser radiation at 1665 and 1667 MHz, detected on 1969 September 2 by Wilson et al. (1972).

3) SiO maser radiation at 86.24 GHz, detected on 1974 March 4 by Kaifu, Buhl, and Snyder (1975).

4) SiO radiation at 43.122 and 42.82 GHz, detected on 1976 June 19 by Balister et al. (1977).

The OH emission of this source at 1665 and 1667 MHz (the so-called main-line frequencies) was monitored from 1969 September to 1972 September by Harvey et al. (1974). During that period it displayed variations in both maser lines, with peak received fluxes of 4 and 6 Jy, respectively.[1] Throughout that period U Ori belonged to a small group of OH sources that emit predominantly in these main-line

[1]However, the data gathered in that experiment are not sufficient to measure the correlation of the OH variations with the optical output.

frequencies, rather than in the 1612 MHz ("satellite") line, as is usually the case for OH radiation from late-type stars. Pataki and Kolena (1974) observed this OH source on 1973 July 28 and November 26, and found it to have the same characteristics as before (i.e., main-line radiation only). But on 1974 May 22 they observed it again, and found it to have changed drastically.

1. The 1667 MHz line disappeared (with measured upper limit of 0.4 Jy).

2. A strong 1612 MHz line emerged, with peak received flux of 22 Jy.

3. No radical change was registered in the output level of the 1665 MHz line, though the spectrum did change.

Almost coincident with this discovery was an attempt on 1974 June 2 by Snyder and Buhl (1975) to detect the 43.122 GHz SiO line in this source. Their reported negative result has an upper limit of 89 Jy, which is equal to the flux that Balister et al. (see above) detected exactly two U Ori periods later.

The flare-up event in the U Ori OH radiation is a unique phenomenon in the observed history of OH masers. It is intriguing for its singularity, as well as for its possible implications for the understanding of OH masers. Is this a regular event in OH masers, but one which we assume to be singular because of our limited data? Does it have any role in the masing process? What can we learn about OH masers in general from the data gathered on this event?

These questions were the motivation for the inclusion of U Ori

in an OH monitoring program, carried out between 1975 July and 1978 March. The results reported in this Letter are an account of the behavior of this maser source following the flare-up event.

II. INSTRUMENTS

The experiment was carried at the Owens Valley Radio Observatory of the California Institute of Technology, utilizing the 40 m altitude-azimuth radio telescope in its fixed prime-focus configuration. The half-power beamwidth of the antenna at 18 cm wavelength is approximately 18'. A linearly polarized feed was used and an unpolarized spectrum was obtained by adding the corresponding spectra of two orthogonal sky polarizations. The receiver, an uncooled parametric amplifier, had a system temperature ranging from 80 to 90 K.

Spectral-line analysis was done with the 100-channel autocorrelator and an off-line Fourier transform run on the IBM 370/158 on the Caltech campus. The autocorrelator was operating in a "total power" mode, alternating every 20 minutes between the source position and an off-source position displaced by 20 R.A. minutes, to minimize baseline distortion. The produced spectra of 250 kHz bandwidth have a velocity resolution of 0.47 km s^{-1} at 1665 MHz. A typical integration time of 80 minutes yielded a temperature sensitivity of 0.035 K, which in this observing configuration corresponds to 0.15 Jy.

Flux calibrations were done with a noise diode in the front end as a reference. Its value was determined by comparison with

3C 348 (Her A), assuming an unpolarized flux of 36.7 Jy at 1666 MHz with spectral index of -1.014 (Kellermann, Pauliny-Toth, and Williams 1969). This calibration procedure is believed to be accurate to within ±5%. This error, deriving mainly from noise-diode output variations and antenna geometrical effects, dominates the absolute uncertainties of the experiment, and consequently will be used as the measurement error.

III. RESULTS

During the observing program the strongest OH lines in U Ori were at the 1612 MHz frequency. Figure 1 shows the 1612 MHz spectrum on 1975 July 15. This early spectrum consists of a sharp feature at -42 km s^{-1} and a group of blended lines peaking at -46 km s^{-1} (see also Reid et al., 1977). Subsequently this spectrum evolved into the one shown in Figure 2, as taken on 1978 January 25. In this spectrum the -42 km s^{-1} feature remained, while the group of blended lines faded and only one sharp feature remained at -47 km s^{-1}.

Figure 3 shows the integrated flux of the U Ori 1612 MHz radiation starting with the first detection by Pataki and Kolena (1974) on 1974 May 24. It remained at an average level of 45 x 10^{-22} W m^{-2} until the beginning of 1976, when it dropped sharply to half its previous level, and proceeded to decline thereafter. Comparing the 1612 MHz intensities with the visual variations, as communicated by the AAVSO (J. A. Mattei 1978, private communication), one can argue that the 1612 MHz output level may be correlated with the stellar cycle.

FIGURE 1

The 1612.231 MHz spectrum of U Ori on 1975 July 15. The unpolarized spectrum is shown with respect to the LSR. The velocity resolution is 0.45 km s^{-1}. This spectrum, obtained approximately 1 year after the 1612 MHz radiation appeared, shows a sharp feature at -42 km s^{-1}, and a group of blended lines peaking at -46 km s^{-1}.

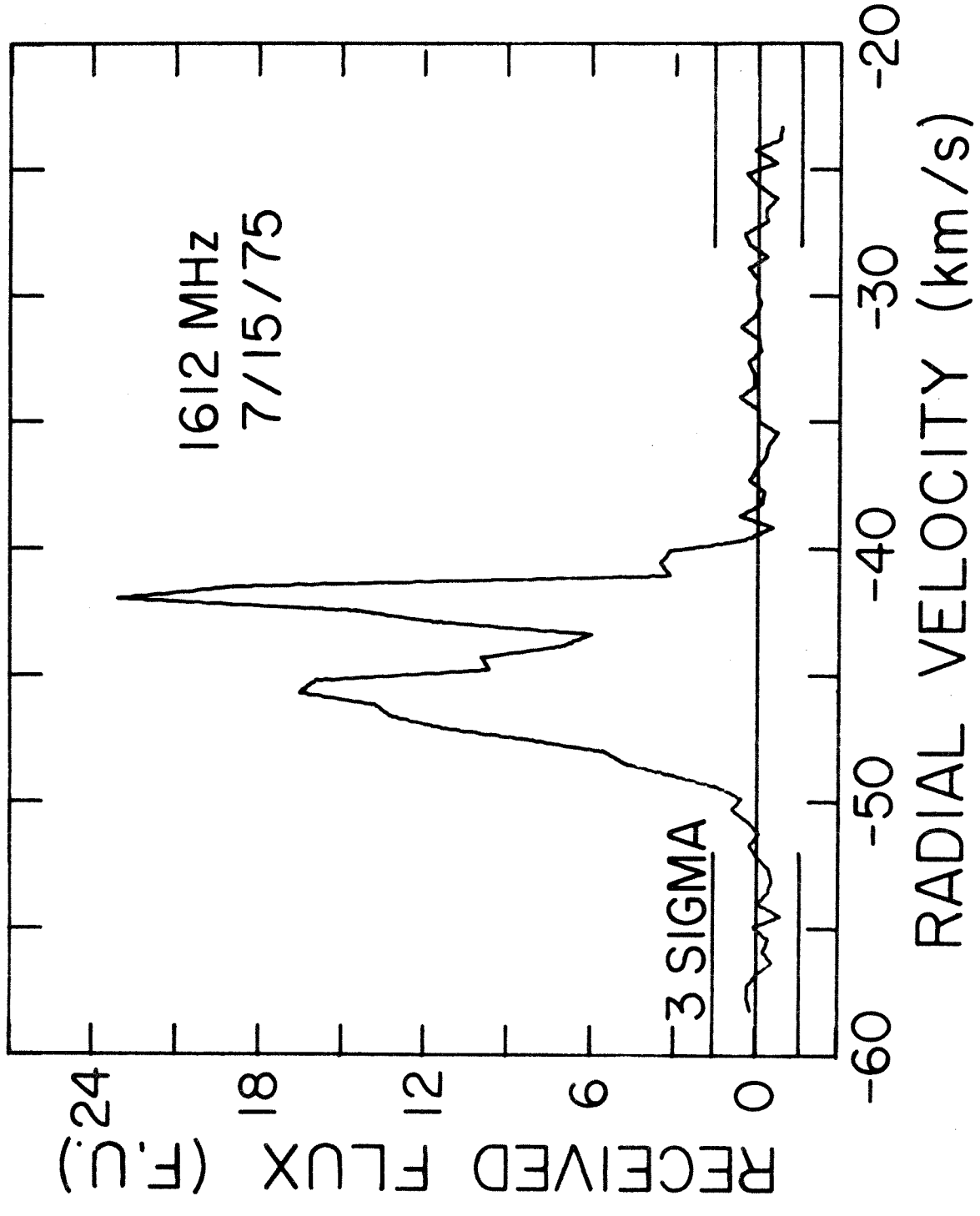
1612 MHz
7/15/75
3 SIGMA
RECEIVED FLUX (F.U.)
0
6
12
18
24
-60
-50
-40
-30
-20
RADIAL VELOCITY (km/s)

FIGURE 2

The OH spectra of U Ori in early 1978. The unpolarized spectra are shown with respect to the LSR. The velocity resolution is approximately 0.47 km s^{-1}. The 1612 MHz spectrum is slightly different from the earlier one shown in Fig. 1. The group of blended lines became clear and a single line remained at -47 km s^{-1}. Also noticeable is the decrease in flux level. The 1667.358 MHz line reappeared and was detected for the first time since it disappeared before 1974 May 22 coincidentally with the emergence of the 1612 MHz lines.

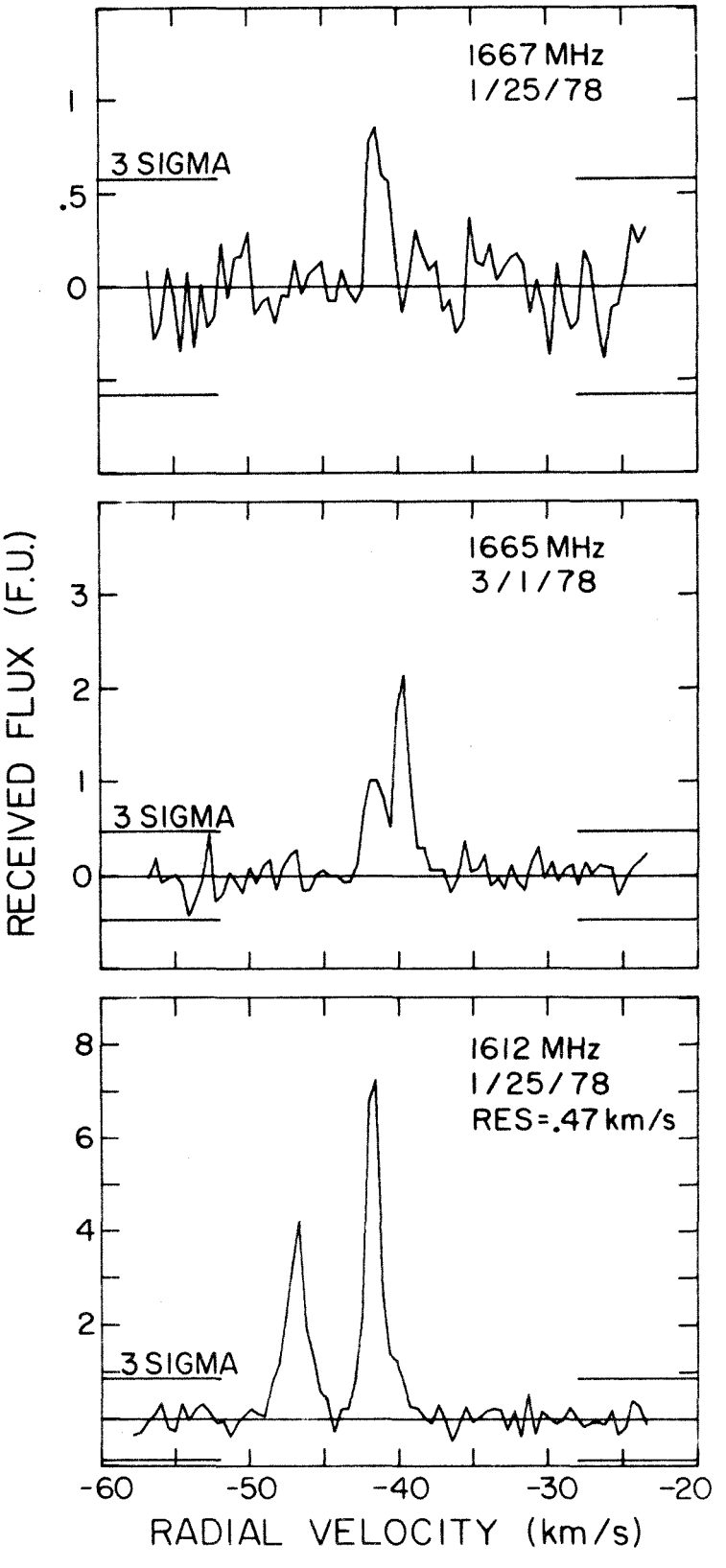
1667 MHz
1/25/78
3 SIGMA
1
.5
0
1665 MHz
3/1/78
3 SIGMA
3
2
1
0
1612 MHz
1/25/78
RES=.47 km/s
3 SIGMA
8
6
4
2
-60
-50
-40
-30
-20
RECEIVED FLUX (F.U.)
RADIAL VELOCITY (km/s)

FIGURE 3

The time variations of the 1612 MHz integrated flux of U Ori, compared with the light curve of the 372 day period, as monitored by the AAVSO (J. A. Mattei 1978, private communication). The first OH point (marked by a cross) is from Pataki and Kolena (1974). The decay in the 1612 MHz output is evident. After 1.5-2 years of strong, probably steady, output, the flux dropped quickly to half of its original level, and continued to decline thereafter. Correlation with the light curve is evident in the last observed stellar period. There is no way to evaluate the variations in the earlier periods.

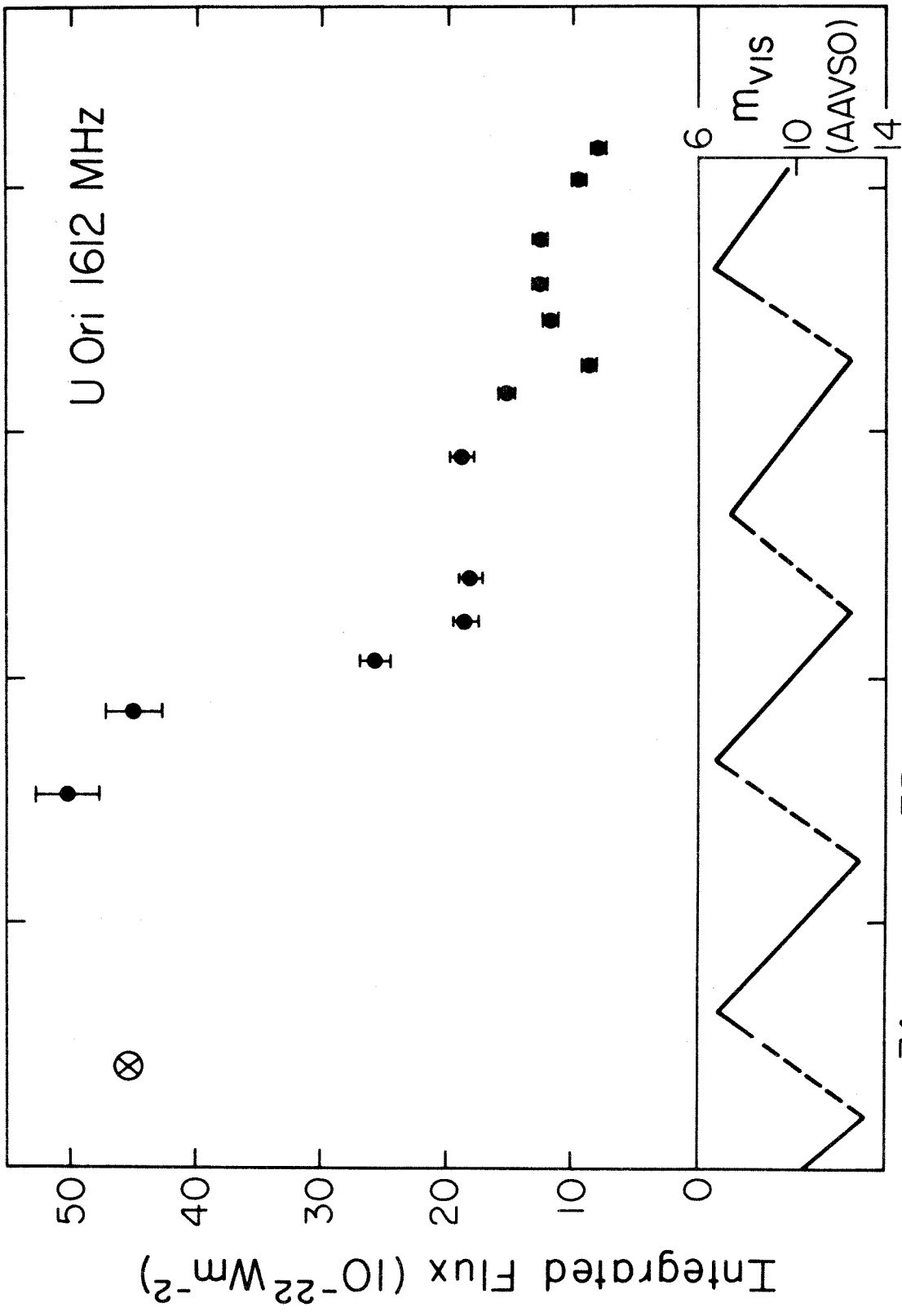
U Ori 1612 MHz
Integrated Flux (10^{-22} Wm^{-2})
0
10
20
30
40
50
m_{VIS}
(AAVSO)
6
10
14
74
75
76
77

There are enough data points only during the last stellar period, and in that case a correlation is apparent. However, the scarcity of 1612 MHz data points, as well as the varying amplitude, make it practically impossible to estimate quantitatively the correlation during the whole observed period.

Because of the weakness of its lines, the 1665 MHz spectrum was not observed as often as the 1612 MHz one. On 1978 March 1 it consisted of two barely resolved lines at -40 and -42 km s^{-1} (Fig. 2). The peak flux of 2.2 Jy in this measurement is about one-half of that observed by Pataki and Kolena (1974) in 1974 May.

The 1667 MHz spectrum, which was not detectable from 1974 May to 1977 June (see Table 1), showed a line on 1978 January 25 at -42 km s^{-1}. Its peak flux was 0.8 Jy.

IV. DISCUSSION

A comparison of the different line velocities in U Ori (Fig. 4) produces three velocity groups. The most distinguished one is the intermediate-velocity group of lines at -42 km s^{-1}. It includes the zero-volt optical absorption, one of the SiO transitions, and an OH line in each of the frequencies and all of the observations. This velocity feature has in three cases a companion feature at -40 km s^{-1}. Lines scattered in velocity around -36 km s^{-1} form the second group. The last is the negative-velocity group which includes the optical emission lines and one of the 1612 MHz features at -47 km s^{-1}.

This multiplicity in line velocities, especially in the OH

FIGURE 4

The velocities of the OH lines observed during this program are compared with each other, with earlier OH lines, and with all other known lines in this source. The velocities indicated are those of the peaks of the lines. The triangle near the bottom represents the group of blended lines as seen in Fig. 1. Three groups of velocities are observed at -47, -42, and -35 km s^{-1}. The first one may be associated with a shock front.

References. (1) Wilson et al., 1972; (2) Kaifu, Buhl, and Snyder, 1975; (3) Balister et al., 1977; (4) Wallerstein, 1973.

U Ori line velocities

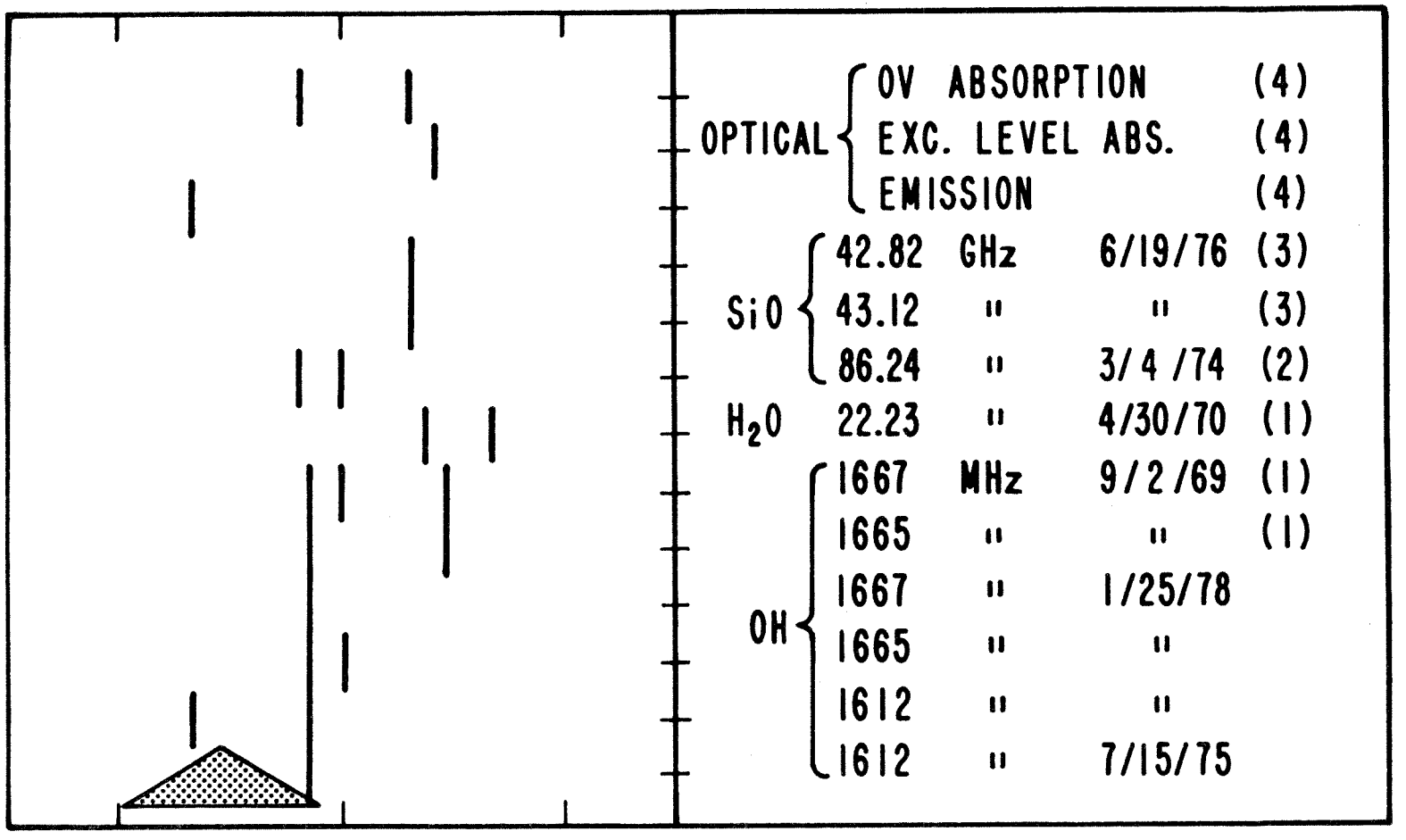

TABLE 1

The 1667 MHz Radiation of U Orionis

Date	Peak Flux (Jy)	Integrated Flux ($\times 10^{-22}$ W m^{-2})	Reference
1969 Sep - 1972 Sep	1-6	1-16	a
1973 Nov 26	>0	>0	b
1974 May 22	<0.4	...	b
1977 Jan 22	<1.0	<0.4	
1977 Jun 15	<0.6	<0.3	
1978 Jan 25	0.8	0.7	

References. [a]Harvey et al., 1974. [b]Pataki and Kolena 1974.

lines, confuses the stellar velocity of U Ori (see Reid, 1976). It also seems to be in conflict with the two-velocity model of OH masers, as developed by Elitzur, Goldreich, and Scoville (1976). That model, which explains the 1612 MHz maser in sources with thick dust shells (e.g., IRC +10011), may be inadequate for U Ori, where the dust shell is very thin. In this case, another pumping process for the 1612 MHz maser may exist in addition to the one that utilizes the dust grains.

Any model of the OH maser in this source has to account for the recent history of the source. Unfortunately, there is very little known about the other molecules and their transition during the studied period.

The 1667 MHz OH lines in U Ori disappeared within a period of 180 days between 1973 November 26 and 1974 May 22. The strong 1612 MHz OH emission was detected for the first time in this source on the later date. This 1612 MHz emission sustained its average output level (allowing for small variations) until about 1975 December.[2] Then, within 100 days, the output level dropped to half, and continued to decline afterward. In early 1978 it dropped to one-fifth of its original output. It seems that while the flare-up event was probably a sudden one, lasting less than 180 days, the reverse process happened within an extended period of several years. Another impression is that the pump mechanisms of the 1612 MHz and the 1667 MHz masers

---

[2]This conclusion is substantiated by measurements shown in Fig. 3, and also by one made by Reid et al. (1977) close to 1975 January 1.

compete in this source. Not only did the appearance of the 1612 MHz lines coincide with the disappearance of their 1667 MHz counterpart, but the 1667 MHz lines reemerged during the lingering decline of the 1612 MHz output.

The event in U Ori could originate from any one of three sources: the central star, the circumstellar envelope, and interstellar space. We assume that the central star is the origin of the event, since it is also the origin of energy and matter in the circumstellar envelope. This assumption is also corroborated by the coincidence in velocity between one of the 1612 MHz lines and the optical emission at -47 km s^{-1} (Fig. 4). The optical emission has been interpreted as the outcome of a shock or MHD wave originating in the subphotosphere of the star (Wallerstein, 1973; Merrill, 1960). The velocity coincidence therefore hints at a possible origin of the recent event in U Ori: a disturbance propagating from the central star into the circumstellar envelope. Another question is whether this disturbance is a short-lived one, or a repeated stimulus sustaining the 1612 MHz radiation? A possible answer to this question comes from the observed evolution of the 1612 MHz spectrum: a large number of velocity features, mostly blended, existed in the early 1612 MHz spectra. This, compared with a cleaner, two-featured spectrum at later dates, may indicate the existence of disorder, maybe even turbulence in the maser environment in the beginning, which subsided later.

Therefore a favored model for the event in U Ori is a short-lived disturbance that propagated from the central star, and excited

the OH maser into its 1612 MHz emitting phase. This excitation relaxed later on a time scale of 2 years, resulting in the decay of the 1612 MHz radiation and the reappearance of the 1667 MHz line. The time limit of 180 days for the beginning of this process has a bearing on the possible nature of the disturbance. Since the change in the OH maser was simultaneous in all velocities, the information should have reached all parts of the maser within a period shorter than 180 days. At what speed should the disturbance propagate then? According to Reid et al. (1977), the apparent size of the OH maser in this source is 10^{15} cm. If all the components of the maser reside in a thin shell concentric with the star, then the speed of propagation does not matter. But if the above symmetry does not exist or the maser has a finite thickness, then the speed of propagation counts. Even if the disturbance had the full period of 180 days to propagate, then it should have traveled faster than 12 km s^{-1} to cover a distance of 2×10^{13} cm. In this case it could not be a shock wave, since a shock wave traveling faster than 12 km s^{-1} will dissipate due to dissociation losses (London, McCray, and Chu, 1977). Therefore we conclude that the OH maser is coupled radiatively to the photosphere. Thus, information about the flare was transmitted to the photosphere as a shock wave, and from there it proceeded with the speed of light to the OH cloud.

CHAPTER II

SUSPECTED ZEEMAN SPLITTING IN THE OH MASERS IN W HYDRAE*

*Submitted to the Astrophysical Journal

ABSTRACT

Observations of the OH maser in W Hya are presented, which suggest an explanation of their unique polarization characteristics. The maser lines may be formed at a distance of $\sim 10^{14}$ cm from the stellar surface in the presence of a magnetic field of ~ 9 milligauss. This magnetic field is coupled to the ionized component of the outflowing circumstellar envelope. In the W Hya case the magnetic field is evident in the strong polarization, Zeeman pattern and differential magnetorotation. However, it may exist unnoticed in other OH sources, and contribute to the pumping mechanism.

I. INTRODUCTION

W Hya is an M-type long-period variable star (LPV). It belongs to a small group of OH sources, which emit predominantly in the 1665/1667 MHz (i.e., mainline) transitions. Wilson et al. (1972) measured the OH spectra of this source in October 1970, with a velocity resolution of .56 km/s. Two features were observed in both mainlines, with respective velocities of 37 and 44 km/s relative to the LSR. A unique characteristic of these spectra is the strong polarization of the maser lines.

Polarization has been observed frequently in OH masers in compact H II regions (e.g., Lo et al., 1975; Moran et al., 1978). However, only few cases are known of polarization in OH masers in LPV. In no other case the degree of polarization approaches the W Hya record of 80%.

This uniqueness of the OH masers in W Hya instigated the detailed study of the source, which is reported here.

II. INSTRUMENTS

The observations were made between July 1975 and March 1978 at the Owens Valley Radio Observatory of the California Institute of Technology.

Most of the measurements were obtained with the 40m altitude azimuth radio telescope, using a room temperature parametric amplifier mounted at the prime focus. One measurement was made with

the 2-element 27m interferometer.

The 40m telescope had a half-power beamwidth at 18 cm wavelength of approximately 18'. A linearly polarized feed was used, and the unpolarized spectra were obtained by adding the corresponding spectra of two orthogonal sky orientations. For obtaining the linear polarization parameters, the spectra were measured in eight different sky orientations spaced equally every 22.5 degrees. The total system temperature ranged from 80 to 90 K.

Spectral-line analysis was done with the 100 channel autocorrelator and an off-line Fourier transform was obtained on the IBM 370/158 at the Caltech campus. The autocorrelator was operated in a "total power" mode, alternating every 20 minutes between the source position and an off-source position displaced by 20 RA-minutes, to minimize baseline distortion. The spectra of 62.5 kHz bandwidth have a velocity resolution of 0.11 km/s at 1665 MHz. A typical integration time of 80 minutes yielded a temperature sensitivity of 0.07 K, which in this observing configuration corresponds to 0.3 Jy.

The position angle (P.A.) and the degree of linear polarization were obtained for each channel by a best fit of the intensities measured for the 8 different sky orientations to

$$A^2 + B^2 \cos^2(\theta - \text{P.A.})$$

Thus the degree of linear polarization is given by

$$B^2/(2A^2 + B^2)$$

Flux calibrations were made using a reference noise diode mounted in the receiver package. Its value was determined by comparison to 3C 348 (HER A), assuming an unpolarized flux of 36.7 Jy at 1666 MHz with spectral index of -1.014 (Kellermann, Pauliny-Toth, and Williams, 1969). This calibration procedure is believed to be accurate to within 5%. This error, deriving mainly from noise-diode output variations and antenna geometrical effects, usually dominates the absolute uncertainties of the experiment. In a few cases, where the maser output is quite small ($<5\times10^{-22}Wm^{-2}$), the receiver noise dominates the uncertainty.

The 27m interferometer was used on 8/15/77 to obtain the circular polarization data of W Hya. This interferometer consists of two movable radio telescopes on rail tracks. Each one has a 27m equatorially mounted antenna with a room temperature parametric amplifier mounted at the prime focus. The half power beamwidth for the 27m telescopes at 18 cm wavelength is approximately 26'. In this experiment the two dishes were located along an east-west baseline, separated by 200'. This separation is sufficiently small that W Hya can be regarded as a point source. A linearly polarized feed was used in each front-end. These rotatable feeds were used either parallel to each other for calibration purposes, or perpendicular to each other to obtain the circular polarization data. A detailed explanation of this method is given by Morris, Radhakrishnan, and Seielstad (1964). The receiver system temperatures were around 90 K.

The two IF signals at 10 MHz were passed through a 24 channel

filter bank of 1 kHz resolution, and were then correlated. The fringes were artificially set at the rate of 60 cycles per minute. They were recorded on magnetic tape and reduced off-line at the Caltech campus. The resulting circular polarization spectra of 48 kHz bandwidth (obtained by alternating between two different local oscillator settings) have a velocity resolution of 0.18 km/s at 1667 MHz. The total integration time of 375 minutes yielded a temperature sensitivity of 0.01 K, which in this system corresponds to 0.1 Jy.

An hour by hour calibration of flux and phase was performed using 3C 273 and 3C 287 as references. Those in turn were flux calibrated against 3C 348 (see above) using the system noise as a reference. The overall phase calibration was achieved by a best-fit solution of the geometric baseline and frequency dependence of the system to measurements of a well established set of point sources. The sense of circular polarization was checked by observing W49.

Two kinds of errors, other than that originating from the Gaussian noise, exist in this experiment. One is a calibration error assumed to be 5%. The other is an error caused by a coupling of the linear polarization to the circular polarization whenever the two feeds deviate from perpendicular. Two measures were taken to minimize this error. One was to determine the real perpendicular setting of the feeds, rather than using the nominal one, by minimizing the fringe amplitude of a circularly unpolarized calibrator. The other measure was the use of sky orientations 30 and 120 degrees for the feeds. These values are close to the linear polarization position angle at the

center of the features, and thus their coupling factor was minimized.

III. RESULTS

Figure 1 shows the 18 cm spectra of W Hya on 7/15/75 during a visual maximum. In the 1667 MHz spectrum two features are apparent at 35.2 and 36.8 km/s. The low-velocity feature (denoted "LO") with peak received flux of 27 Jy seems to be slightly asymmetrical, having a high velocity tail. The second feature ("HI") has a peak received flux of 33 Jy and appears to be symmetrical. The 0.5 km/s half power width of HI is a bit narrower than that of LO. A trace of a third line seems to exist. Extended between 38.3 and 39.2 km/s, this suspected line has a received flux of 1-1.5 Jy, comparable to the 3 sigma error level of the measurement. A possible confirmation to this third line can be seen in Figure 3, in the spectrum taken on 8/15/77, which was also obtained during a visual maximum. Here the suspected line appears at 38.4 km/s and shows in a single filter in the interferometer measurement.

The 1665 MHz spectrum of 7/15/75 is dominated by a line at 37 km/s with 14 Jy received flux. This line appears to be almost coincident in velocity and shape to the 1667 MHz HI feature. Here LO is degenerated to a wide deformed line with a small off-center peak at 36.1 km/s with 5 Jy received flux. There is no apparent parallel to the 1667 MHz suspected third line.

The features at 44 km/s, which were reported by earlier workers (see introduction) disappeared.

FIGURE 1

The mainline spectra of W Hya on 7/15/75 during a source maximum. The unpolarized spectra are shown with respect to the LSR. The velocity resolution is 0.11 km/s. In the 1667 MHz spectrum, two strong features at 35.2 and 36.8 km/s plus a suspected third one at 38.6 km/s resemble a Zeeman pattern. No 1612 MHz radiation from this source has ever been detected.

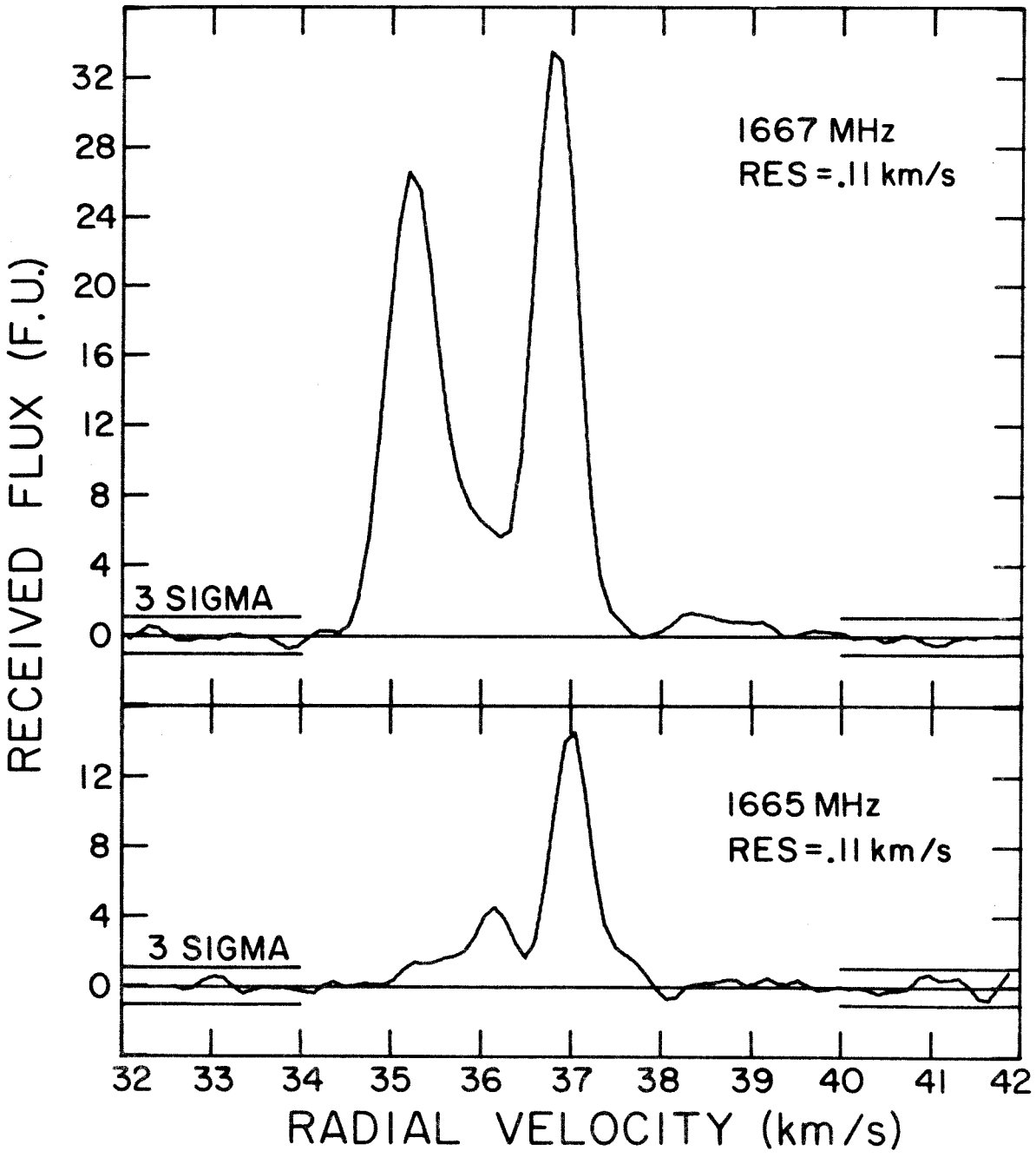
RECEIVED FLUX (F.U.)
32
28
24
20
16
12
8
4
0
1667 MHz
RES = .11 km/s
3 SIGMA
12
8
4
0
1665 MHz
RES = .11 km/s
3 SIGMA
32 33 34 35 36 37 38 39 40 41 42
RADIAL VELOCITY (km/s)

Time variations

The OH output of W Hya, which varies in time by a factor up to 30, had three maxima during the observing period coinciding with the visual maxima. Figure 2 displays the integrated fluxes of the three observed features.[1] The 1667 MHz HI and LO features peak typically at $10\text{-}15\times10^{-22}$ Wm^{-2}. One exception is the 1976 LO output, which rose to only half of that level. In both 1667 MHz curves a secondary maximum is apparent at phase 2/3. The extent of the variations of the two 1667 MHz velocity features is different. While their maximum integrated fluxes are comparable, LO has twice the integrated flux of HI during the secondary maximum, and four times as much at minimum time. So the flux variation of HI between minima and maxima is a factor of 30, while that of LO is a factor of 10 or less. The peak flux of HI is bigger than that of LO during maximum and is smaller during the rest of the cycle.

The 1665 MHz output has a maximum integrated flux of 6×10^{-22} Wm^{-2}. At minimum its level was not detected, with an upper limit of 0.5×10^{-22} Wm^{-2}. In this case the 1976 maximum is only slightly weaker than the previous one, similar to the 1667 MHz HI feature. The 1977 maximum was not measured at its peak during the interferometer experiment. However, it is evident from the 1667 MHz curves that this peak would have been missed in the 1667 MHz curves as well but for the interferometer measurement. The 1665 MHz integrated flux

---

[1]The border between the 1667 MHz LO and HI features is set at 36.2 km/s in calculating the integrated fluxes.

FIGURE 2

The time variations of the integrated flux of the 1667 MHz LO and HI features and the 1665 MHz radiation are compared with the phase 0 arrows separated by 382 days, as computed from visual observations of the AAVSO (1978) and AFOEV (Lépine, 1978). Very narrow maxima are evident, with variations of up to factor 30 between maxima to minima. This indicates the existence of unsaturated masers. The secondary maxima at approximately phase 0.6 are probably real and are paralleled in H_2O data by Lépine (1978).

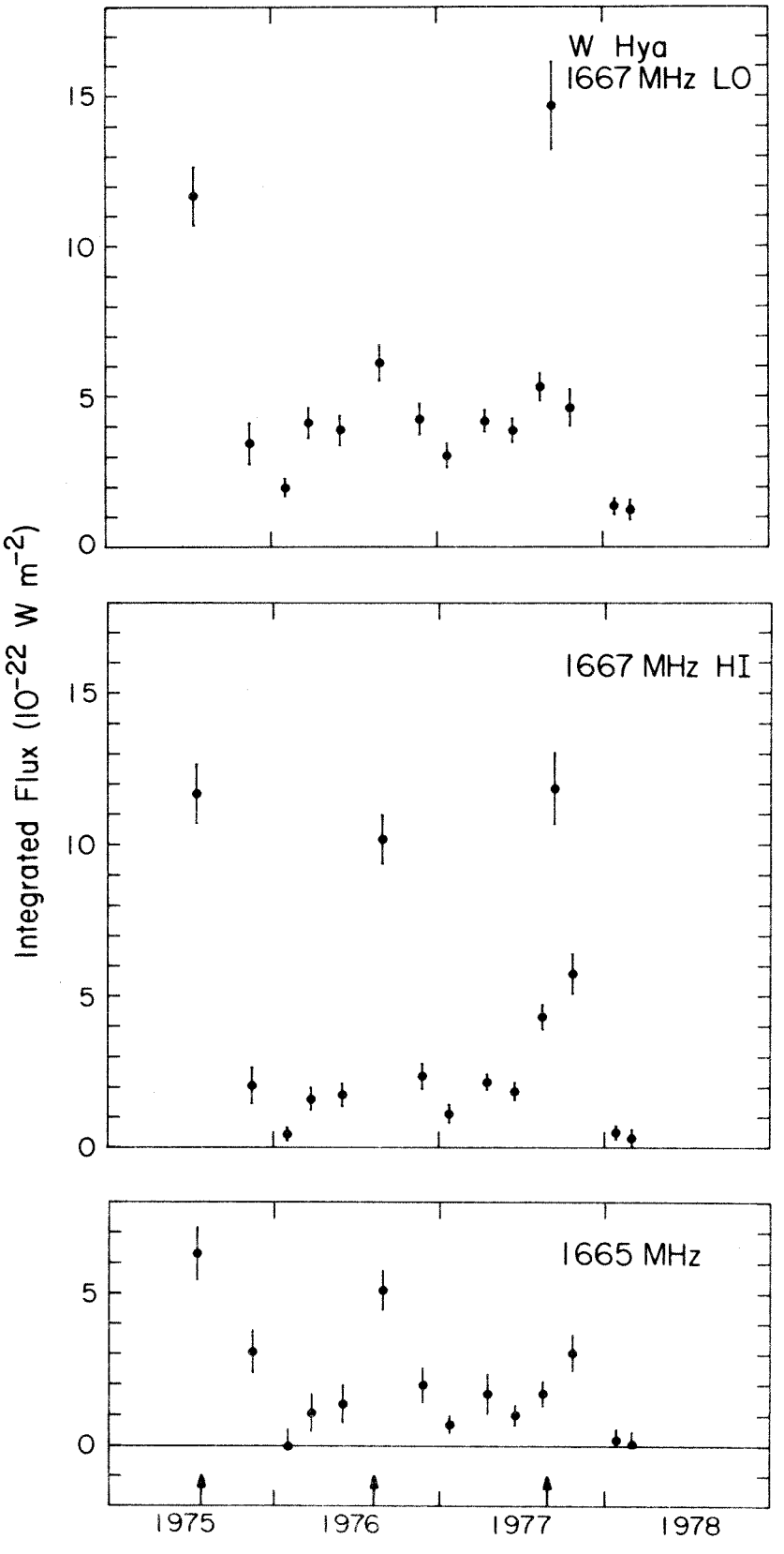
W Hya
1667 MHz LO
1667 MHz HI
1665 MHz
Integrated Flux (10^{-22} W m^{-2})
0
5
10
15
1975
1976
1977
1978

can also be assumed to have a secondary maximum.

Table I lists the results of the cross-correlations performed between any two of the three monitored OH variations, the H_2O variations (Lépine, 1978), and a sine fit to the combined visual data of the American Association of Variable Star Observers (J.A. Mattei, 1978, private communication), and of the Association Française des Observateurs d'Etoiles Variables (communicated privately by Lépine, 1978). The visual data in this case are rather sparse. They are represented in Figure 2 by arrows on the bottom, which correspond to phase 0, with a computational error of 5 days. In the table, the upper right half contains the correlation-factor, while the lower left half contains the phase-difference in days (a positive phase-difference means that the row precedes the column).

It must be noted that in the W Hya case, the correlation values are dominated by the maxima of the OH curves, since most of the maser output is emitted during that limited portion of the cycle. Therefore, the shape and timing of these peaks are critical to this analysis.

The best estimate of shape can be given for the 1977 peak, whose half power time span is equal to or less than 55 days. In that case, the 8/15/77 measurement preceded the visual maximum by approximately 10 days, while the OH output had just started to rise towards the peak. One can also notice that the 7/15/75 measurement is within the error limits of the visual maximum, and the recorded OH output is already peaking.

Some interesting qualities are apparent in comparing the OH

Table I

THE CORRELATION BETWEEN OH H_2O AND VISUAL VARIATIONS

	I	II	III	IV	V
			CORRELATION-FACTOR		
I	*	0.89	0.72	0.71	0.75
II	-1.5	*	0.87	0.82	0.67
III	-20.5	-13.0	*	0.75	0.66
IV	-3.0	+17.5	+27.5	*	0.63
V	-27.0	-40.5	-0.5	-30.5	*
			PHASE-DIFFERENCE (DAYS)		

I - 1667 MHz LO

II - 1667 MHz HI

III - 1665 MHz

IV - VISUAL

V - H_2O

data with that of the H_2O. The weakness in the 1976 maximum of the 1667 MHz LO feature is paralleled in the H_2O case. Here the maximum has about one quarter of the strength of the neighboring maxima. The secondary maxima are evident in this case. And finally, the time duration of the maximum output is approximately 120 days, more than twice as long as the upper estimate of the OH case.

Polarization

Table II lists the linear polarization parameters of the 1667 MHz radiation as recorded on 4 different occasions. The position angle and the degree of linear polarization are given for the peaks of the two features and on their wings (the term "right wing" will be used for the high velocity wing of a feature, to prevent confusion). Notably, the position angle of LO varies significantly within the feature, while that of HI is less variable within the feature. LO has 13% linear polarization, while HI has as much as 39% linear polarization on 7/15/75, during a maximum in the OH output level. The degree of linear polarization is higher in the center of HI than in its wings, which is not necessarily the case for LO.

The four dates of observation, 7/15/75, 3/23/76, 6/1/76, and 4/15/77 correspond roughly to phases 0, 2/3 (secondary maximum), 5/6, and again 2/3. The data taken on 3/23/76 seem to be of lesser quality than that of the other three dates. The position angle of the peaks of the features varies from date to date on a scale of 10 degrees. The strongest linear polarization was recorded on 7/15/75, as mentioned. The apparent tendency of the P.A. to decrease with

Table II

THE LINEAR POLARIZATION OF W HYDRAE AT 1667 MHz

vel.	7/15/75		3/23/76		6/1/76		4/15/77	
	P.A.	lin. pol.	P.A.	lin. pol.	P.A.	lin. pol.	P.A.	lin. pol.
km/s	degrees	%	degrees	%	degrees	%	degrees	%
34.75	152.4± 8.1	10.6±3.1	156.5± 5.1	35.7±10.1	155.4±12.7	30.7±14.6	151.3±27.0	10.5±10.2
35.20*	121.2± 2.7	13.8±1.2	124.3± 1.2	25.0± 1.5	136.1± 1.3	13.8± 0.5	127.8± 3.1	12.1± 1.2
35.65	105.6± 6.1	13.4±3.0	118.8±28.0	24.5±33.3	130.0± 2.7	19.8± 2.0	112.2± 5.3	10.8± 2.0
36.10	92.7±16.2	7.4±4.5	94.9± 7.4	27.3±10.2	176.9± 1.7	18.6± 1.1	90.0±49.6 ±	9.8± 8.8
36.45	28.1± 1.4	34.6±2.0	179.6± 8.0	31.8±13.5	21.1±17.8	26.0±17.2	43.0±15.8	13.9± 8.0
36.80*	29.9± 1.3	39.4±2.0	15.4±17.4	34.0±32.0	20.0± 3.5	32.1± 4.2	24.6± 2.3	27.5± 2.5
37.15	34.6± 4.5	33.3±5.6	17.9±32.6	15.7±22.3	14.1± 3.3	16.0± 1.9	21.1± 3.4	18.1± 2.4

*Peak of feature

increasing velocity within LO is broken on one occasion, that is on 6/1/76, when the P.A. turns upwards on the right wing.

The difference between the average P.A. of LO and HI ranges from 90 to 110 degrees. Notably on 7/15/75, during maximum output, the P.A. difference is very close to 90 degrees.

The linear polarization of the suspected third feature was measured with suitable accuracy only on 7/15/75. The result, not recorded in the above table, at (38.6±0.3) km/s the P.A. is (83±7) degrees, and the degree of linear polarization is (30.0±7.5) %.

The circular polarization, as measured on 8/15/77, is displayed in Figure 3. The sense of circular polarization is opposite for LO and HI. In both cases the circular polarization is apparently a wing phenomenon. In LO the degree of circular polarization in both wings is about 5%, twice as much as in the peak. In HI a degree of circular polarization as large as 13% is recorded in the left wing, while at the peak of the feature and towards the right wing it is strongly decreasing.

For the 1665 MHz spectrum only one polarization measurement is given, that of the linear polarization on 7/15/75 (Table III). The degree of linear polarization measured in the HI feature is uniquely high, up to 76%. LO also has a high degree of linear polarization, up to 40%. The position angle of HI is quite close to that of the 1667 MHz HI feature, while the value of 1665 MHz LO is distinctive.

Table III

THE LINEAR POLARIZATION OF W HYDRAE AT 1665 MHz

	7/15/75	
vel. km/s	P.A. degrees	lin. pol. %
35.50	56.5±18.4	27.7±18.1
36.15*	52.2± 8.8	40.2±13.2
36.65	25.5± 1.8	76.4± 5.1
37.00*	24.8± 1.8	75.6± 5.7
37.35	23.3± 1.4	68.9± 4.0

*Peak of feature

FIGURE 3

The 1667 MHz spectrum of W Hya on 8/15/77, also during a source maximum. In the upper portion of the figure, the unpolarized spectrum is shown with respect to the LSR. The velocity resolution is 0.18 km/s. The lower portion of the figure shows the circular polarization divided by the total received flux. Stronger wing polarizations are probably the result of transfer effects, which are also responsible for the magnetorotation of the linear polarization.

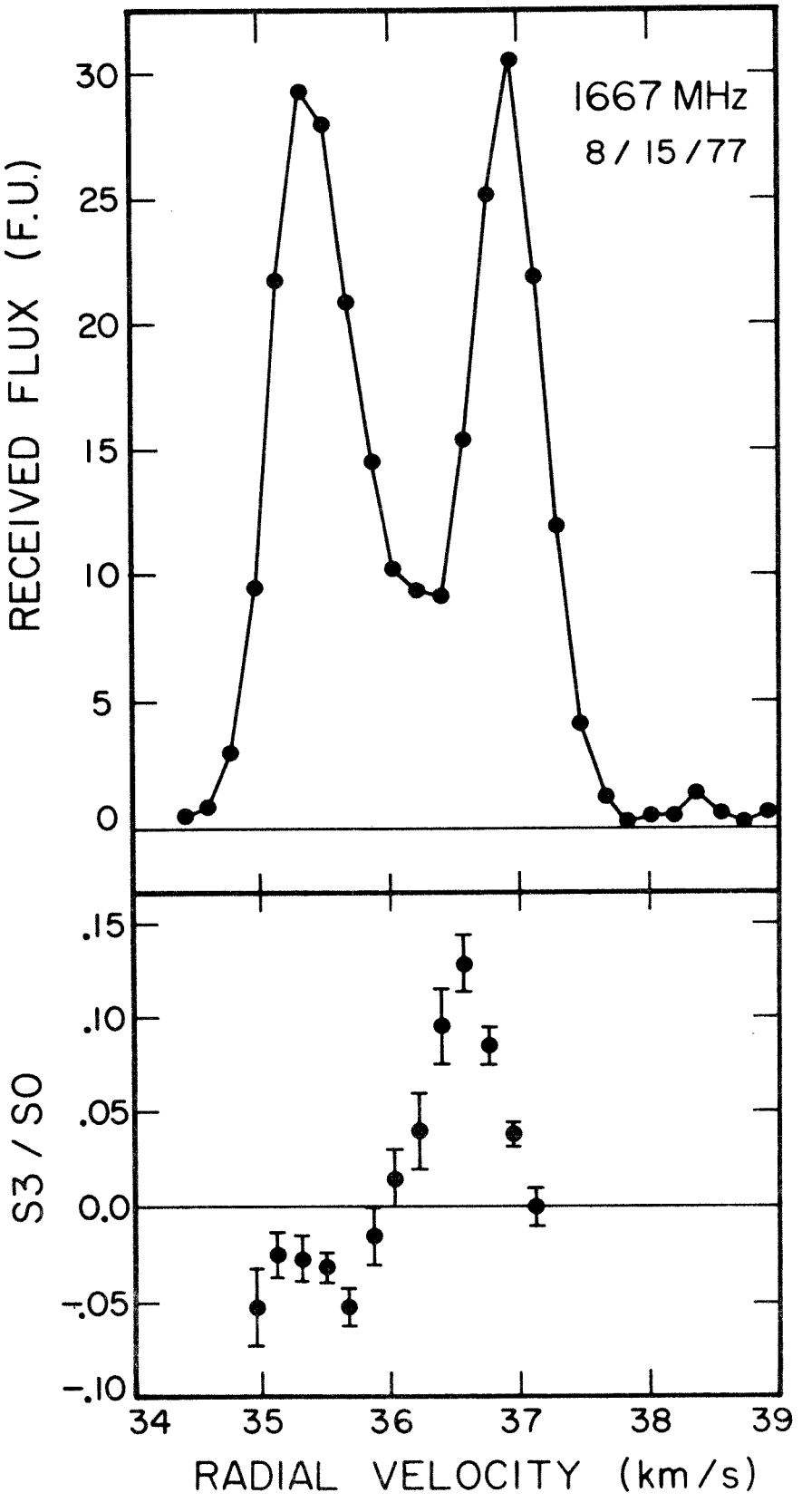
1667 MHz
8 / 15 / 77
RECEIVED FLUX (F.U.)
30
25
20
15
10
5
0
S3 / S0
.15
.10
.05
0.0
-.05
-.10
34
35
36
37
38
39
RADIAL VELOCITY (km/s)

IV. DISCUSSION

Two characteristics of the OH masers in W Hya are quite unique for a late-type-variable: the high degree of polarization and the strong variations in the output level. The strong variations in the output level may indicate that the masers are unsaturated. The flux variations of a saturated maser reflect the changes in the pumping rates, and those are not believed to vary by the big factor observed here. Regarding the correlations of the various variations, a more detailed monitoring of the OH maser at maximum time is necessary. It is obvious that in this case the relationship between the stellar radiation and the OH variations is more complicated than a linear one. Since no model for the OH output level exists, it is not known how often it ought to be sampled. For this reason no error estimates are given for the correlation values in Table I, and the reader is advised to treat the results with care. A qualitative observation of the correlation values reveals that the visual maximum coincides with the beginning of the OH and H_2O maxima. However, in both masers the high output level is sustained for an extended time past the visual maximum. The H_2O maximum lasts longer than the OH one.

The polarization phenomenon is explained by the introduction of magnetic fields. It is not mandatory that these fields be of significant strength, and well ordered throughout the circumstellar envelope. It is possible that the polarization is produced in the portions of the maser closer to the star, and then is amplified by the rest of the maser which extends farther away from the star.

The reason for the uniqueness of this phenomenon may very well be intrinsic to the source. It can also be caused because our line of sight happens to be in a preferred alignment, such as is the W Hya equatorial plane.

The Zeeman pattern hypothesis

A very tempting interpretation of the polarization of W Hya uses the Zeeman pattern. One can assume that there are three features in the 1667 MHz spectrum, corresponding to the σ^+, π, and σ^- components. Thus HI could be the π component. Its polarization would then be purely linear and its frequency unshifted. LO and the small third feature would then be the two σ components, displaced in frequency in opposite senses by the magnetic field. Their polarizations should be eliptical with the linear orientation perpendicular to that of HI. The circular senses should be opposite.

The best supporting fact for the Zeeman hypothesis is the difference between the P.A. values at the peaks of the LO and HI features which is close to 90°. Since we need not assume that the maser emission of the different features originates from the same location in the circumstellar cloud, a deviation from perpendicular can be accounted for by different orientations of the magnetic field in the two locations. An explanation for the degeneracy of the third feature is easy, and follows an argument by Cook (1966): As the distance from the star increases, the magnetic field decreases.

That will have opposite effects on the apparent velocity of the two σ components. That with higher apparent velocity will decrease in apparent velocity, and vice versa. But increasing distance also results in increasing kinematic velocity (see Goldreich and Scoville, 1976). Therefore the σ component with lower apparent velocity will have these two effects compensating for each other and will thus end up with a larger optical depth. The opposite will happen to the other σ component, resulting in a lower optical depth and therefore a much smaller gain.

For the Zeeman hypothesis to be consistent with the data, we have to be convinced that the circular polarization of HI is non-existent. In Figure 3 a somewhat strong circular polarization exists in the left wing of this feature, though it falls off to zero towards the right wing. This contradicts the Zeeman pattern hypothesis, unless it can be explained otherwise.

The magnetic field

If indeed the Zeeman pattern hypothesis is correct, and assuming that the 1667 MHz HI and LO features originate at the same location (which need not be the case), then the Zeeman shift of 1.6 km/s corresponds to a magnetic field of 9.1×10^{-3} gauss (Palmer and Zuckerman, 1967). It is also required that the discriminating effect, which enhances LO and suppresses the other σ component, occurs. For this to happen, the gradient of the Zeeman shift must be of comparable magnitude and opposite sign than the gradient of the Doppler shift.

The conditions on the magnetic field at the maser location are therefore:

$$B = 9.1 \times 10^{-3} \text{ gauss}$$

and

$$\frac{dB}{dr} = -5.7 \times 10^{-8} \frac{dv}{dr}$$

The geometry of the magnetic field in the source is unknown, and one can only try to infer it from the observed data. From the fact that the π component is observed, one can deduce that there is a component of the field in the location of the maser, that is perpendicular to our line of sight. Furthermore, from the fact that the linear polarization in this source is much stronger than the circular polarization, we learn that the component of the magnetic field that is perpendicular to our line of sight is much stronger than the parallel one.

One can also consider the state of ionization in the circumstellar cloud and its possible effect on the magnetic field. Any substantial ionization in the vicinity of the maser would cause strong Faraday rotation, and so destroy the linear polarization of the maser radiation. In this case one can calculate an upper limit of 10^3 cm^{-3} for the electron density in the vicinity of the maser. On the other hand, an electron density of few cm^{-3} is sufficient in this case to freeze in the magnetic field to the outflowing gas (Kaplan and Pikelner, 1970).

Therefore it is assumed that in the vicinity of the maser $3<N_e<10^3$ cm^{-3}, and the field lines are dragged by the gas.

Transfer effects

The occurrence of differential rotation in the linear polarization can be attributed to transfer effects. These effects are treated by Goldreich, Keeley, and Kwan (1973). In addition to magnetorotation, these effects are capable of producing circular polarization in a beam that has originally been purely linearly polarized. This may be the explanation for the existence of circular polarization in the wing of HI, even though the Zeeman hypothesis cannot account for it. It may also be the explanation for the changes in polarization since the measurements by Wilson et al. (1972).

V. CONCLUSION

The introduction of magnetic fields into the OH masers in LPV stars has been also suggested by Reid et al. (1979). Their estimates of the strength of the fields is compatible with this work.

The existence of relatively strong magnetic fields, as well as that of unsaturated masers, indicate that the W Hya OH masers reside close to the stellar surface. A distance of $1\text{-}2\times10^{14}$ cm is conceivable. This proximity of the maser to the stellar surface may be implying that direct stellar radiation is pumping the maser. The enhancement of one of the sigma components in the Zeeman pattern, which is demonstrated in this case, may have an essential role in the

direct stellar pumping. While making the maser transitions optically thick in spite of the velocity gradient, it does not effect the optical depth of the IR transitions, which are thin because of the velocity gradient.

The author believes that two different pumping mechanisms of OH masers occur in LPV stars. One is a direct radiative pumping by stellar radiation, which is responsible for masers located close to the star. The other is pumping by FIR radiation from dust grains, located farther away from the star, where the velocity gradient is very small (Elitzur, Goldreich, and Scoville, 1976). In the W Hya case, the second mechanism does not produce observable maser radiation because its dust shell is too thin.

CHAPTER III

OH MASER PUMPING BY LINE BLOCKAGE AT 2.8 MICRONS*

*Coauthored with N. Z. Scoville; to be submitted to the Astrophysical Journal

ABSTRACT

The pumping of OH masers in late-type-variables by direct stellar radiation of 2.8μ is studied. Two pumping schemes are suggested based on line coincidences between OH V=0-1 transitions and strong H_2O ν_3 transitions. The water molecules perturb the stellar radiation by absorption, and thus cool the coinciding OH transition. It is demonstrated that this cooling is capable of producing strong OH masers in the circumstellar envelopes of late-type-variables. This model can account for the existence of mainline ($\Delta F=0$) OH masers, which is hard to explain otherwise.

I. INTRODUCTION

The OH masers in the circumstellar envelopes of late-type-variables has been observed in three frequencies: 1612, 1665, and 1667 MHz (see Figure 1). The fourth possible transition at 1720 MHz has never been observed in these sources, but does exist in other interstellar masers. Theories of the satellite line masers (those at 1612 and 1720 MHz, as opposed to mainline masers at 1665 and 1667 MHz) usually utilize the discriminatory effect of selection rules on radiative transitions between the hyperfine sublevels, and thus on the population flow. This manipulator does not exist in the mainline maser theory. In that case there is a full symmetry between the two sublevels of the lambda doublet. This symmetry combined with the proximity in the energy levels of the lambda doublets fails most attempts to form a straightforward model of radiative pumping for the mainline masers.

One way around is to consider non-radiative processes like collisions, chemical reactions, etc. Another is to devise a scheme in which the above symmetry is broken. This second approach was taken by Litvak (1969) who suggested the overlapping of hyperfine sublevels in IR transitions, caused by turbulence of the OH molecules, as the reason for pumping. Also Evenson et al. (1970) proposed that the pumping of the OH molecules is performed by resonant FIR (Far Infrared) radiation emitted by a water laser (and so, by no means simplifying the problem).

This paper presents a scheme based on coupling of NIR (Near

FIGURE 1

The ground level of the OH molecule is divided by Λ-doubling and by hyperfine splitting into four sublevels. The four resulting 18 cm transitions are divided to two mainlines ($\Delta F=0$), and two satellite lines ($\Delta F=1$). Though all four lines have been detected in maser emission from celestial sources, the explanation of the mainline masers has been elusive so far.

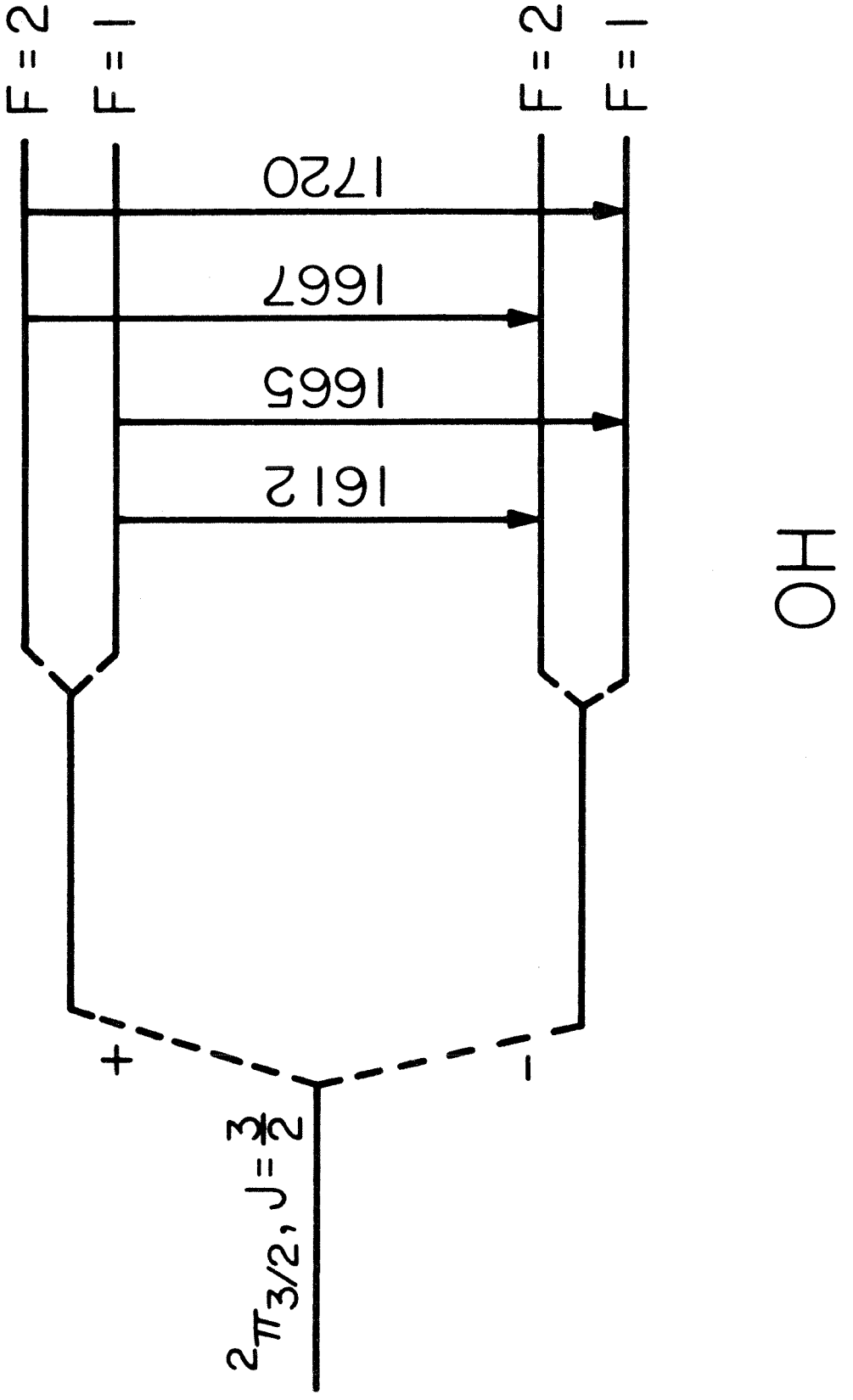
F = 2
F = 1
F = 2
F = 1
1720
1667
1665
1612
OH
+
-
$^2\Pi_{3/2}, J=\frac{3}{2}$

Infrared) radiation from the central star with the OH molecules, and the perturbation of the radiation field by water molecules in interior shells of the circumstellar envelope closer to the star. Its feasibility is tested by a model of the circumstellar envelope that was developed by Goldreich and Scoville (1976). At this stage of preliminary work the hyperfine structure is neglected, and therefore only a simplified single mainline exists.

II. THE PUMP MODEL

a) Principles of the pumping mechanism

We suggest two pumping schemes for the OH mainline masers. Both are based on possible frequency coincidence between V=0-1 OH transitions and transitions in the ν_3 band of the water molecule. In the circumstellar cloud, NIR photons from the central star at 2.8μ wavelength excite the OH molecule from the ground state into the first vibrationally excited level (V=1). The molecule then radiatively decays and cascades back to the ground level. In our case, the NIR radiation is perturbed by water molecules residing in its path. Absorption by optically thick ν_3 water transitions happens to mask the NIR frequency that corresponds to the V=0-1 transition from the upper lambda sublevel of the OH ground state. The net result is a population flow from the lower to the upper lambda sublevels. This flow, if strong enough, will result in population inversion and masering.

b) The pump cycles

Figure 2 shows a part of the OH $^2\pi_{3/2}$ ladder (not to scale).

FIGURE 2

OH rotational levels in the $^2\pi_{3/2}$ ladder are shown which are radiatively connected to the ground state. The ground state (V=0, J=3/2) is coupled radiatively with two rotational states (J=3/2, 5/2) in the first vibrationally excited state (V=1). These in turn are coupled radiatively with three rotational states (J=3/2, 5/2, 7/2) in the ground vibrational state (V=0). The energy spacings are not drawn to scale and hyperfine splitting is omitted. The number k is a running number for the energy levels, and not a quantum number.

FIGURE 3

The energy levels are the same as in Figure 2. In this scheme some of the stellar radiation in the 2-7 transition frequency is blocked. This figure shows the net result in the collisionless approximation. An excess of population flow in the 1-8-4-2 cycle is created, relative to that in the cooled 2-7-3-1 cycle. The result is the pumping of the 1-2 maser.

FIGURE 4

Here the 2-10 transition is cooled by the blocking of the stellar radiation. The net result, in the collisionless approximation, is a population flow from the k=1 to the k=2 levels.

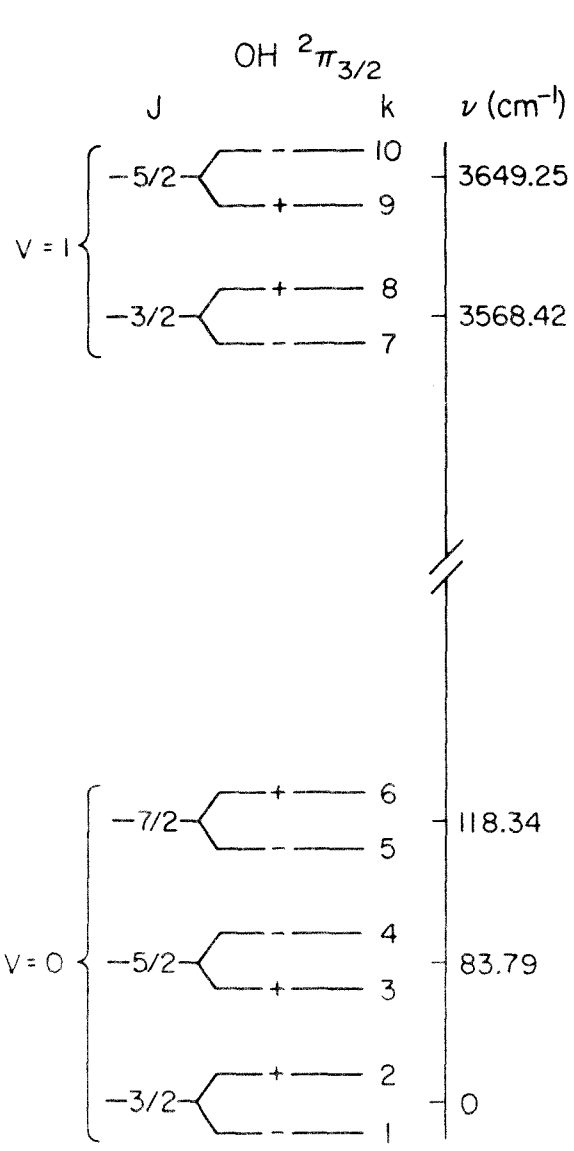
OH $^2\pi_{3/2}$
J
k
ν (cm^{-1})
V = 1
−5/2
10
9
3649.25
−3/2
8
7
3568.42
V = 0
−7/2
6
5
118.34
−5/2
4
3
83.79
−3/2
2
1
0

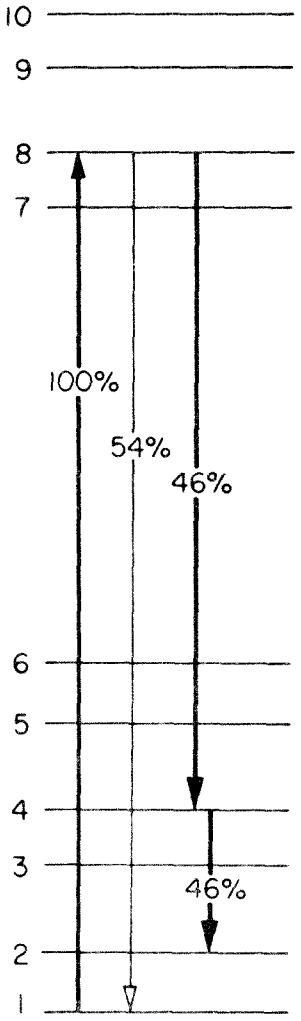
OH PUMP CYCLE
SCHEME I
10
9
8
7
6
5
4
3
2
1
100%
54%
46%
46%

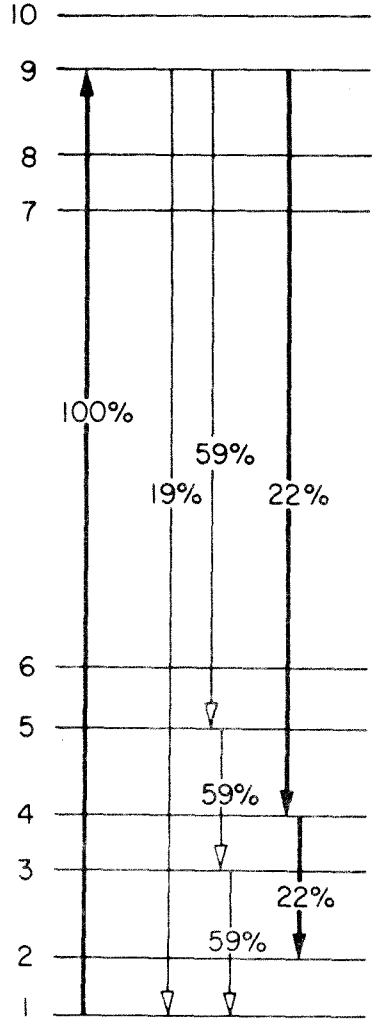
OH PUMP CYCLE
SCHEME II
10
9
8
7
6
5
4
3
2
1
100%
19%
59%
22%
59%
59%
22%

The levels are designated by a number k according to rising energy. Hyperfine structure is ignored in this discussion, and thus both mainline transitions are represented by a single transition k=2-1. The ground level is radiatively coupled by electric dipole transitions to two rotational levels (J=3/2 and 5/2) in the first vibrationally excited state (V=1), and those in turn are coupled to three V=0 rotational levels (J=3/2, 5/2, and 7/2). The selection rule being $\Delta J=0, \pm 1$, and $+ \leftrightarrow -$. The $^2\pi_{1/2}$ ladder is insignificant to this argument since downward transitions from V=1 states into V=0, $^2\pi_{1/2}$ states are much weaker than the ones into the V=0, $^2\pi_{3/2}$ states. The relevant IR transitions are listed in Table I with their respective frequencies and Einstein A coefficients. Two of these transitions are nearly coincident in frequency with strong water vapor ν_3 transitions.

Coincidence I: At approximately 3568.3 cm^{-1}. The OH transition with spectroscopic designation $Q_1(3/2^+)$ (k=2-7 in Figure 2) has a frequency of 3568.28 cm^{-1} according to Dieke and Crosswhite (1962).[1] The corresponding H_2O transition is the ν_3 (0,0,1) $6_{24} \leftrightarrow$ (0,0,0) 7_{25} one at 3568.290 cm^{-1} (Camy-Peyret et al., 1973). This line is extremely strong, and its optical depth in the circumstellar cloud can be higher

---

[1]There are no direct measurements of this line's frequency. The quoted frequency was obtained indirectly from UV measurements. Model calculations based on molecular constants yield the values 3568.4204, and 3568.4216 cm^{-1} (Maillard, Chauville, and Mantz, 1976; Maillard, 1978), and 3568.41 cm^{-1} (Destombes, 1978a, 1978b).

TABLE I

OH RADIATIVE TRANSITIONS

k"→k'	V"→V'	J"→J'	±"→±'	ν(cm^{-1})	A (s^{-1})
3-1	0-0	5/2-3/2	+→-	83.70[1]	0.1[3]
4-2	0-0	5/2-3/2	-→+	83.87[1]	0.1[3]
5-3	0-0	7/2-5/2	-→+	118.20[1]	0.5[3]
6-4	0-0	7/2-5/2	+→-	118.47[1]	0.5[3]
7-2	1-0	3/2-3/2	-→+	3568.28[1]	10.557[4]
7-3	1-0	3/2-5/2	-→+	3484.74[2]	9.168[4]
8-1	1-0	3/2-3/2	+→-	3568.55[2]	10.557[4]
8-4	1-0	3/2-5/2	+→-	3484.59[2]	9.168[4]
9-1	1-0	5/2-3/2	+→-	3649.25[1]	3.791[4]
9-4	1-0	5/2-5/2	+→-	3565.28[2]	4.256[4]
9-5	1-0	5/2-7/2	+→-	3447.30[2]	11.723[4]
10-2	1-0	5/2-3/2	-→+	3649.25[1]	3.791[4]
10-3	1-0	5/2-5/2	-→+	3565.68[1]	4.256[4]
10-6	1-0	5/2-7/2	-→+	3447.00[2]	11.723[4]

References: (1) - Dieke and Crosswhite 1962; (2) - Maillard et al. 1976; (3) - Burdyuzha and Varshalovich 1973; (4) - Mies 1974.

than one (Flaud and Camy-Peyret, 1975, 1978).[2] If a coincidence indeed occurs, and the two transitions overlap in frequency, then part of the stellar NIR output is blocked from the OH molecules by the water molecules residing in inner shells. This situation of a deficiency of radiation in the k=2-7 transition can equivalently be treated as if the OH molecules are exposed to an excess of radiation in the k=1-8 frequency. The population flow in this scheme is shown in Figure 3. Molecules excited to the k=8 level will spontaneously decay to levels k=1 and k=4 with corresponding Einstein A coefficients of 10.6 and 9.2 s^{-1} (Mies, 1974). From level k=4 the molecules will further decay into level k=2. It means that about one half of the excessive NIR radiation in the k=1-8 transition (as compared to k=2-7) will amount to population flowing from the k=1 to the k=2 sublevels.

Coincidence II: At approximately 3649.2 cm^{-1}. The OH transition with spectroscopic designation $R_1(3/2^+)$ (k=2-10 in Figure 2) has a frequency of 3649.25 cm^{-1} according to Dieke and Crosswhite (1962).[3]

---

[2]It is surprising to find that a third abundant molecule has a transition in the same frequency. It is the H_2 molecule's $1 \leftrightarrow 0$ $O_1(3)$ quadrupole transition at 3568.222 cm^{-1} (Brannon et al., 1968). However, this transition is very weak, with $A=4x10^{-7}$ s^{-1} (Beckwith, 1978), and will not be considered for the OH maser.

[3]See remark (1). The model values here are: 3649.3376, and 3649.3459 cm^{-1} (Maillard, Chauville, and Mantz, 1976; Maillard, 1978), and 3649.33 (Destombes, 1978a, 1978b).

The corresponding H_2O transition is the (0,0,1) $4_{04} \leftrightarrow$ (0,0,0) 5_{05} at 3649.283 cm^{-1} (Camy-Peyret et al., 1973). This line is also extremely strong (Flaud and Camy-Peyret, 1975, 1978). In this case the coincidence will be equivalent to an excess of radiation in the k=1-9 frequency. The population flow in this scheme is shown in Figure 4. Molecules excited to the k=9 level will spontaneously decay to levels k=1,4, and 5 with corresponding Einstein A coefficients of 3.8, 4.3, and 11.7 s^{-1} (Mies, 1974). From level k=5 most of the molecules will cascade down to k=1, but those from level k=4 will decay into level k=2. This means that about 22% of the excessive NIR radiation in the k=1-9 transition will amount to population flowing from k=1 to k=2 sublevels.

III. THE TEST MODEL

In order to test these schemes under the physical conditions in the circumstellar cloud, we used a model for the envelope structure developed by Goldreich and Scoville (1976). In the model, the central star has a luminosity of 10^4 $L_\odot$, a surface temperature of 2000 K, and a radius of 5.9×10^{13} cm. It is losing mass at a rate of $3 \times 10^{-5} M_\odot$ yr^{-1}. Dust grains, which nucleate in the outer atmosphere, are accelerated away from the star by radiation pressure. They transfer momentum to the gas by collisions with the gas molecules. The result is a radially outflowing cloud with the velocity characteristics described in Figure 5.

The abundance of OH molecules calculated in the model (see

FIGURE 5

The velocity of the circumstellar gas as calculated by Goldreich and Scoville (1976) is used in the test model of the proposed pumping mechanisms.

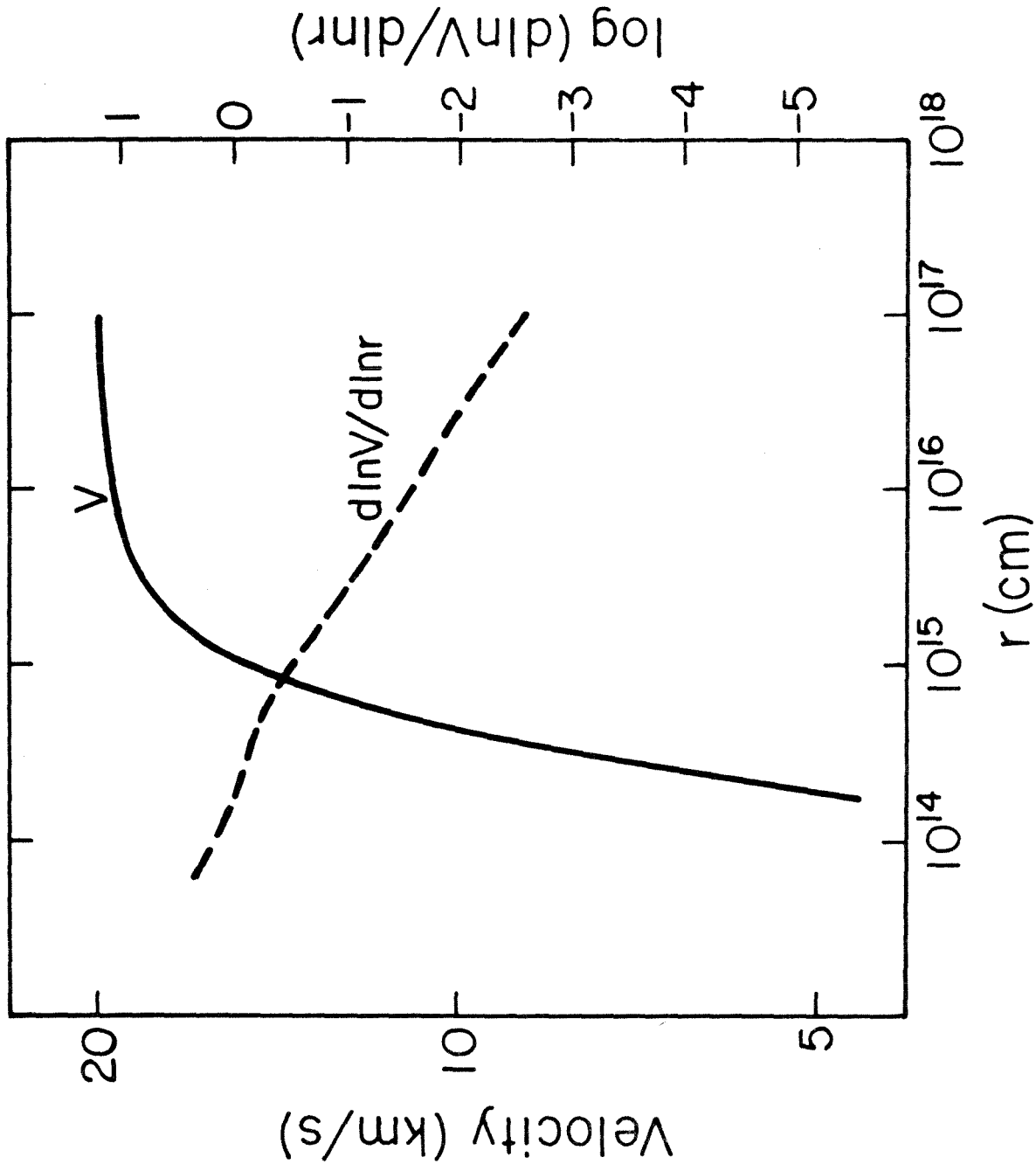
Velocity (km/s)
20
10
5
log (dlnV/dlnr)
1
0
-1
-2
-3
-4
-5
r (cm)
10^{14}
10^{15}
10^{16}
10^{17}
10^{18}
V
dlnV/dlnr

FIGURE 6

The densities of the OH and H_2 molecules in the circumstellar envelope are taken from Goldreich and Scoville (1976). The model calculations show that the maser output is sensitive to the ratio of the OH to H_2 densities.

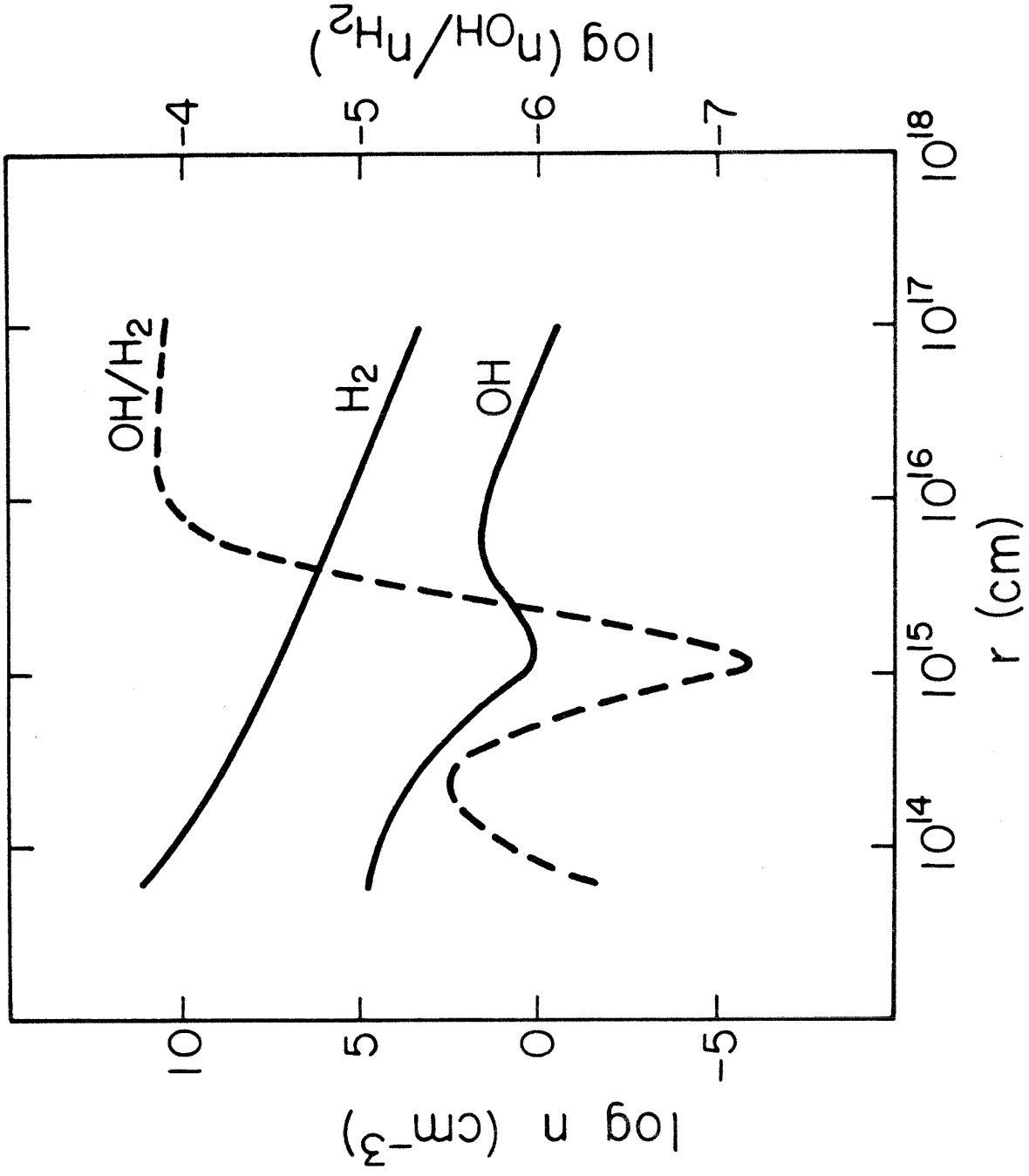
log (n_OH/n_H2)
-4
-5
-6
-7
OH/H2
H2
OH
10
5
0
-5
log n (cm^-3)
10^14
10^15
10^16
10^17
10^18
r (cm)

Figure 6) is controlled by chemical exchange reactions and by dissociation of H_2O molecules. The reaction $OH + H_2 \leftrightarrow H_2O + H + 0.69$ eV, which has an activation energy of 0.3 eV, rapidly converts OH molecules into H_2O molecules in the warm ($T \gtrsim 500°K$) inner ($r \leqslant 2 \times 10^{15}$ cm) region of the circumstellar envelope. At high temperatures OH is also destroyed by the reaction $OH + H \leftrightarrow O + H_2 + 0.3$ eV which also has an activation energy of 0.3 eV. Beyond $r \approx 2 \times 10^{15}$ cm, T is so low that the exchange reaction is slow compared to the expansion time scale; at this point the OH and H_2O relative abundances become frozen. In the outer region of the circumstellar envelope, OH molecules are produced from the photodissociation of H_2O molecules by interstellar ultraviolet radiation and from the dissociation of H_2O molecules by collisions with dust grains.

The collisions with dust grains are the dominant source of heat input to the circumstellar gas. The major sources of cooling are the emission of infrared radiation by H_2O molecules undergoing vibrational decay (at $r < 10^{15}$ cm) and rotational decay (at $r > 10^{15}$ cm) and adiabatic expansion (at $r > 10^{16}$ cm). The gas temperature decreases from 2000 K near the stellar surface to 800 K at $r = 10^{15}$ cm and to 100 K at $r = 10^{16}$ cm. At $r > 10^{15}$ cm the temperature falls approximately as $r^{-3/4}$.

The rate equations governing the OH level populations were solved for statistical equilibrium using escape probabilities formalism for the radiative transfer. The treatment is identical to that employed by Elitzur, Goldreich, and Scoville (1976) to test their model for

FIR pumping of the OH 1612 MHz maser in the same stars. The computer program that calculates the conditions in the OH maser incorporates the above physical conditions through the following factors:

1) Three kinds of transitions between energy levels are experienced by the OH molecules: spontaneous emission, stimulated absorption/emission, and collisional transitions.
2) The OH molecules are radiatively excited by the diluted black body radiation from the central star. In the NIR, this direct stellar radiation dominates the contribution from the relatively cool grains local to the region of OH masing.
3) One NIR transition is partially obscured by H_2O. It is either the 2-7 or the 2-10 transitions. The degree of obscuration is a parameter of the calculation which is indicated by the proportion of stellar radiation that reaches the OH cloud.
4) Another obscuration of the stellar radiation is caused by the finite optical depth of the OH IR transitions themselves.
5) The emissivity at the maser frequency is calculated as the amplification of the spontaneous emission; no background source is assumed. The effects of maser saturation are included in the solution of the rate equations and in calculating the output emissivity.

At present there exist no reliable calculations for collisional

excitation of OH by H or H_2. In view of this uncertainty in the detailed form of cross sections we chose to adopt a simple form for collisional deexcitation rates

$$\langle \sigma v \rangle_{ul} = 7 \times 10^{-13} \, g_1 \sqrt{T} \qquad cm^3 \, sec^{-1}$$

where g_1 is the statistical weight of the final lower state. The upward rates are given by the detailed balance condition as

$$\langle \sigma v \rangle_{lu} = \langle \sigma v \rangle_{ul} \, \frac{g_u}{g_1} \, e^{-E/kT}$$

The adopted forms for the collision rates have the virtue that they are "neutral" with respect to the doublet levels and thus any inversion occurring in the solutions cannot be due to cross section peculiarities. At low temperatures the vibrational deexcitation rates due to H and H_2 are small compared to the elastic scattering rates (Millikan and White, 1963). We have therefore neglected all collisions between vibrational states.

IV. RESULTS AND DISCUSSION

Figures 7 and 8 show the results of the model calculations of the OH masers in the circumstellar cloud for the two pumping schemes. The quantity calculated is the emissivity, which is the rate of photons emitted per cm^3 per sec as a function of distance from the star. In each case two different obscuration values are used, one in which only 1/4 of the stellar radiation in the obscured transition is reaching the OH

FIGURE 7

The calculated emissivity in the maser transition using the first scheme. Two values of stellar radiation in the perturbed line (2-7) are used. High emissivity exists in two zones, the "near zone" around $r=2\times10^{14}$ cm, and the "far zone" around $r=3.5\times10^{15}$ cm. The low emissivity at $r=10^{15}$ cm is correlated with the low value of n_{OH}/n_{H_2} (see Figure 6).

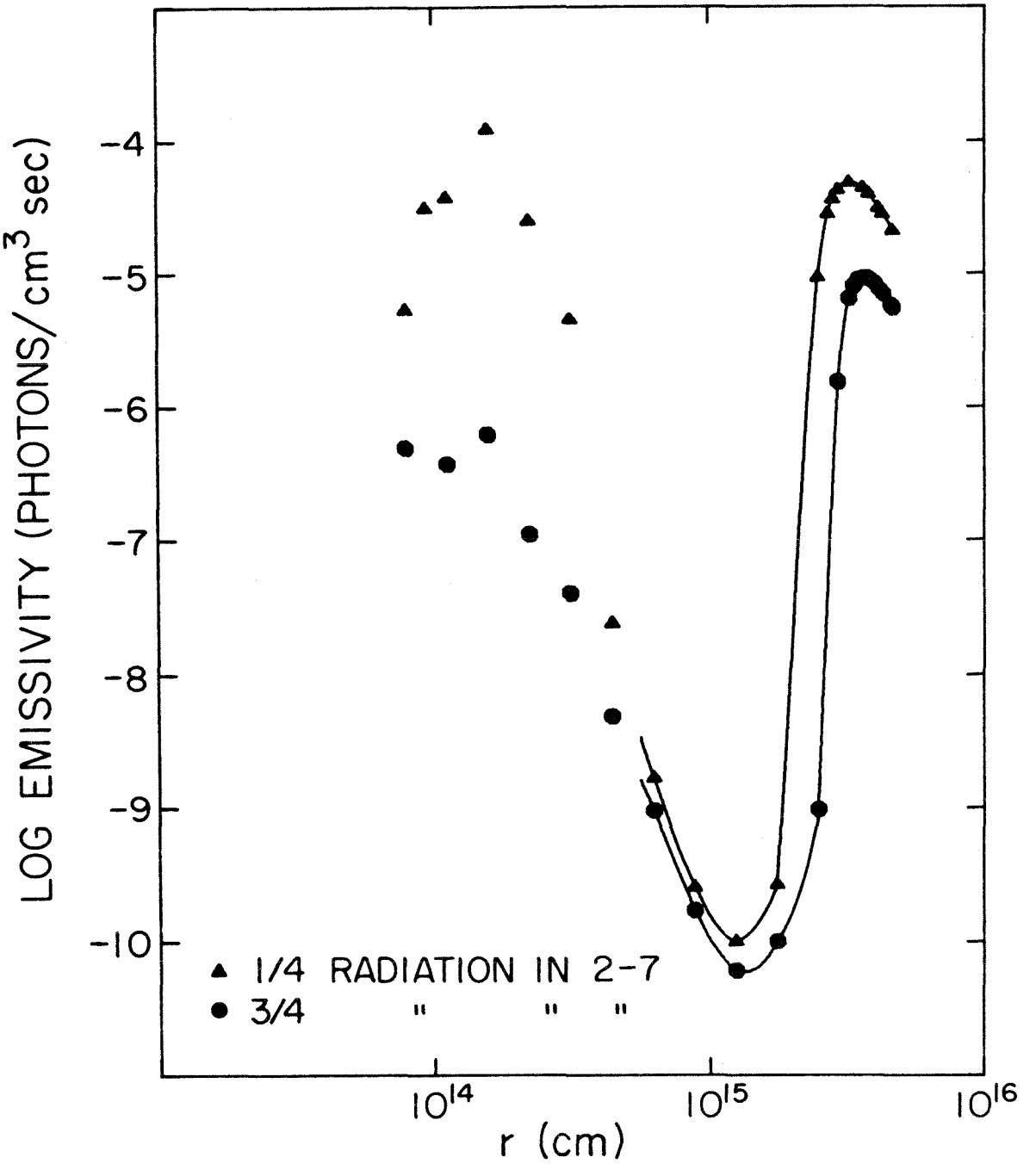
LOG EMISSIVITY (PHOTONS/cm³ sec)
-4
-5
-6
-7
-8
-9
-10
▲ 1/4 RADIATION IN 2-7
● 3/4 " " "
10¹⁴
10¹⁵
10¹⁶
r (cm)

FIGURE 8

The result in the case of the second pumping scheme is very similar to that in the first one. The emissivity in the far zone is weaker by a factor of 2, but that in the near zone is stronger in this case.

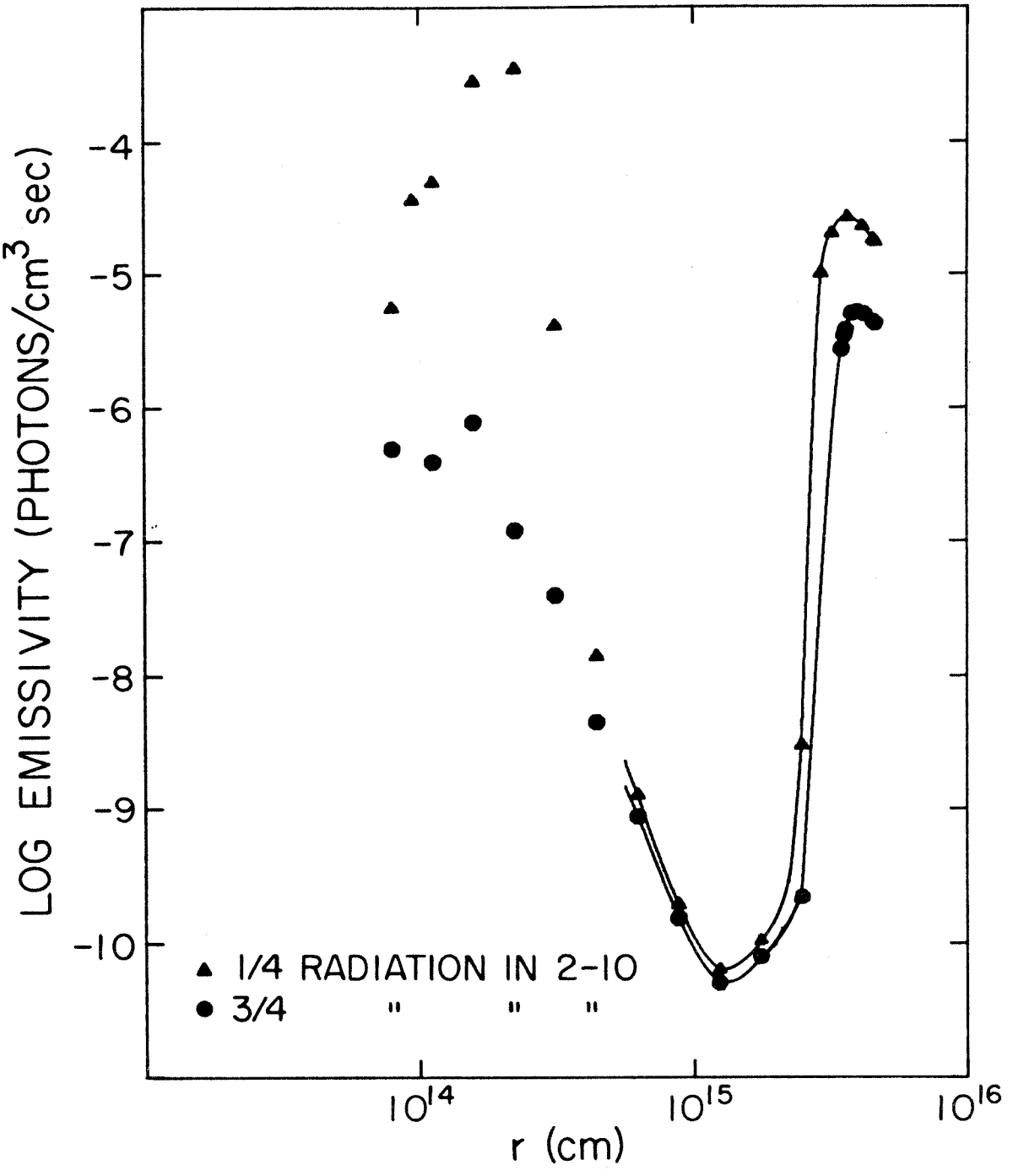
LOG EMISSIVITY (PHOTONS/cm^3 sec)
-4
-5
-6
-7
-8
-9
-10
▲ 1/4 RADIATION IN 2-10
● 3/4 " " "
10^{14}
10^{15}
10^{16}
r (cm)

molecules, and in the other 3/4. In all cases, the existence of two high emissivity zones is evident. Centered at $r = 2 \times 10^{14}$ cm and $r = 3.5 \times 10^{15}$ cm respectively, these zones are separated by a low emissivity zone around $r = 10^{15}$ cm. In the near zone, the emissivity varies from 10^{-6} to almost 10^{-3} photons cm^{-3} sec^{-1}. The variation in the far zone is much smaller. It is approximately one order of magnitude around the mean value of 10^{-5}. The difference in the emissivity between the two schemes is very small, limited to roughly a factor of two in all cases. The first scheme produces stronger maser emission in the far zone, and it is the other way around in the near zone.

The total photon rate of the OH maser can be calculated from the emissivity by multiplication by $4\pi r^2 \Delta r$. An emissivity of 10^{-5} could account for the observed photon rate of 10^{42} sec^{-1} in either of the high emission zones, if a big enough maser length exists. The needed lengths are 2×10^{17} cm in the near zone, and 6.5×10^{14} cm in the far zone. The demand can be met rather easily in the far zone, while it seems to be off by three orders of magnitude in the near zone. The prospects for a strong enough maser in the near zone cannot be written off. Firstly, the emissivity can be stronger than 10^{-5} by two or more orders of magnitude given sufficient blocking. This is especially true in the second pumping scheme (see Figure 8).

The OH population inversion is established by quite different routes in the near and far zones. In the outer region the inversion route in both schemes follows very closely the simple model discussed

in section II, and shown schematically in Figures 3 and 4. That discussion based entirely upon considerations of radiative processes is essentially a complete description in the outer zone.

In the near zone the population inversion occurs due to a combination of both radiative and collisional processes. Here the proximity of the stellar surface means more pumping radiation, but at the same time the collision rates go up. Also in the shell at $8x10^{13} < r < 6x10^{14}$ cm the OH abundance is high. The latter circumstance causes the OH infrared transitions to become optically thick and therefore a general decrease in the rates of infrared pumping relative to those of collisions. With transitions 2-7 obscured close to the star, level 7 will be underpopulated and with transition 2-10 obscured, level 10 is underpopulated. In the presence of a high collision rate close to the star where n_{H_2} is large and radiative decay is reduced due to high opacities, collisions within the V=1 state will tend to shift population towards the underpopulated levels (7 and 10 respectively). Lastly, level 2 gains population by radiative decay directly in either 7-2 or 10-2. In agreement with this explanation we note that the IR transitions (e.g., 1-8) become optically thick inside $3x10^{14}$ cm which is close to the outer boundary of the near zone maser.

The maser conditions at $r=3.5x10^{15}$ cm are analyzed in Tables II, III, and IV. The population distributions of the OH molecule is listed in Table II for all the four calculated cases. It is evident that in all cases the population inversion is

TABLE II

POPULATION DISTRIBUTION AT $r=3.5\times10^{15}$ cm

k	1	2	3	4	5	6	7	8	9	10
2J+1	3	3	5	5	7	7	3	3	5	5
x					10^{-3}	10^{-3}	10^{-7}	10^{-7}	10^{-7}	10^{-7}
1/4 (2-7)	.389	.391	.100	.101	9.17	9.23	4.05	8.67	4.19	4.18
3/4 (2-7)	.389	.391	.101	.101	9.27	9.24	7.14	8.67	4.19	4.19
1/4 (2-10)	.390	.392	.101	.100	9.25	8.82	8.68	8.65	4.18	2.12
3/4 (2-10)	.389	.391	.101	.101	9.29	9.10	8.68	8.66	4.18	3.51

TABLE III

EXCITATION TEMPERATURES AR $r=3.5 \times 10^{15}$ cm

(°K)

	1-2	3-4	5-6	2-7	3-7	2-10	3-10	6-10
1/4 (2-7)	-16	-21	-98	373	404	382	414	496
3/4 (2-7)	-18	-77	246	389	423	382	414	496
1/4 (2-10)	-17	41	14	395	430	364	393	467
3/4 (2-10)	-19	92	31	395	430	377	408	488

	1-3	2-4	3-5	4-6	1-8	4-8	1-9	4-9	5-9
all	89	89	71	71	395	430	382	414	496

TABLE IV

THE PUMP CYCLE AT $r=3.5 \times 10^{15}$ cm

(TRANSITION RATES IN 10^{-4} cm^{-3} sec^{-1})

	1→8→4	2→7→3	1→9	2→10	4→9	3→10	9→5→3	10→6→4	4→2	3→1 net	1→2 coll.*	maser
1/4 (2-7)	.58	-.18	1.07	1.07	.12	.11	1.18	1.18	1.64	.89	.75	.29	.47
3/4 (2-7)	.58	.33	1.06	1.07	.12	.12	1.18	1.18	1.64	1.39	.25	.16	.09
1/4 (2-10)	.58	.58	1.07	.16	.11	.36	1.18	.52	.99	1.41	.25	-.01	.26
3/4 (2-10)	.58	.58	1.07	.77	.12	.20	1.18	.96	1.43	1.56	.08	.05	.03

* collisions

very small because the maser is saturated.

In the far zone, the OH/H_2 density ratio is maximal. Its high value, combined with the low gas temperature, is the reason for the high emission rate. Here the small velocity gradient along the radial direction helps in forming an optically thick maser transition. But at the same time it causes the pumping IR transitions to become optically thick. The falloff in emissivity at $r=4x10^{15}$ cm is due to both the increasing opacity of the relevant OH IR transitions as the velocity gradient decreases and the decreasing IR pump rate due to increased distance from the star. Since the emissivity falls faster than r^{-2} at large r, the maximum flux observed from this model would arise from the peak at $3.5x10^{15}$ cm. The total output of the model near this peak is $1\text{-}2x10^{42}$ maser photons per second, in good agreement with rates deduced for observed sources (Wilson, Barrett, and Moran, 1970).

Coincidence considerations

The difference in rest frequencies between the OH and the H_2O transitions range according to the various estimates from -1 to +11 km/s in the first coincidence, and from -2.5 to +5.5 km/s in the second. Such differences can be compensated by the kinematics of the circumstellar envelope. If the H_2O and OH molecules both have the velocity pattern described in Figure 5, then the H_2O absorption line will be seen by the OH molecules as red shifted. In that case a coincidence will happen only if the H_2O line rest frequency is higher than the OH line. If instead the H_2O line has a lower frequency, then

the H_2O molecules have to be moving towards the OH molecules, for the coincidence to happen. This can occur if the outward motion of inner shells of the circumstellar envelope is faster than that of the outer shells, as suggested by Lépine, Paes de Barros, and Gammon (1976). Otherwise, special kinematics are required.

The frequency of the 1-8 transition is higher by 11 km/s than that of the 2-7 transition, and the frequency of the 1-9 transition is lower by 11 km/s than that of the 2-10 transition (Maillard, Chauville, and Mantz, 1976; Maillard, 1978). These differences are big enough compared to the thermal velocities ($\sim$ 1 km/s) to assure that only one of any competing pair of transitions (e.g., 1-8 vs. 2-7) can be obscured.

It is conceivable that the line blockage is caused by the OH molecule itself. For example, when the outer envelope is moving with about 11 km/s greater outflow velocity than the inner shell, the OH 2-7 line in the outer envelope can be blocked by the 1-8 transition from closer to the star. Comparing this blocking of OH by itself with the blocking by water vapor, it is felt that the latter will be a more likely effect due to the higher abundance of H_2O and the larger line strength for the H_2O transitions. Since in both cases, blockage by OH and H_2O, it is the same transitions 2-7 and 2-10 that are perturbed, all the excitation analysis presented in the previous section carry directly over to the case of blockage by OH.

The role of the stellar radiation at $\lambda = 18$ cm

In the calculations presented above the stellar radiation at $\lambda = 18$ cm was not taken into account. This is justified if there is no maser component in our line of sight towards the star. If, however, there is such a component, its effect on the low velocity emission peak can be calculated in the same manner that it is done by Elitzur, Goldreich, and Scoville (1976). In the case of 1/4 of the stellar radiation in the 2-7 transition the optical depth at $r = 3.5 \times 10^{15}$ cm is -1.35. The fraction of the total flux in the low-velocity emission peak that is contained in this component of small angular diameter is close to 1, compared to ~ 0.5 for the model of Elitzur, Goldreich, and Scoville (1976).

Since very little has been done so far in resolving mainline masers in LPV stars, we cannot evaluate the model on this ground. It is, however, worthwhile to mention that Elitzur, Goldreich, and Scoville (1976) found their model for the 1612 MNz masers to be contradictory to the observations in this respect. Another aspect of this result is that the low-velocity emission peak should be stronger than the high-velocity one, particularly if the maser is unsaturated. Two supporting cases for this prediction are known: W Hya (see chapter II), and R Aql (Wilson and Barrett, 1972). However, a

more detailed examination of the available mainline data is necessary in order to reach a sound conclusion.

V. CONCLUSIONS

The idea of line coincidence as the cause of maser pumping is not new. Litvak (1969) has also used it for the OH masers (see the introduction above). Geballe and Townes (1974) used it to explain the SiO masers.

It seems that if any of the coincidences discussed above indeed occur, then this model can account for the observed OH masers at distances comparable to $r = 3.5 \times 10^{15}$ cm. An explanation of the OH masers in the base of the circumstellar envelope most probably can be furnished by this model, if the physical conditions are somewhat more favorable than the ones used in our calculations. In both cases, if no other factors interfere, the mainline masers will prevail, since the natural line strengths are bigger by an order of magnitude than that of the satellite lines. However, the combination of this pumping mechanism with the one suggested by Elitzur, Goldreich, and Scoville (1976) can produce strong 1612 MHz masers.[4] As a matter of fact, the need for such a combination is mentioned in the quoted work.

It is conceivable that this pumping mechanism could explain

---

[4] In comparing the two models, one notices that in the 1612 MHz maser model radiation occurs at 3×10^{16} cm, while in the mainline model discussed here the radiation occurs at 3×10^{15} cm. This difference is in good agreement with spectral and VLBI data (e.g., Reid and Muhleman, 1978).

the OH masers at the edge of compact HII regions as well. The required ingredients in that case include a strong enough continuum source at 2.8μ. Also, some constraints must be made on the dust grains in the maser environment since they cannot obscure the continuum source from the OH molecules.

REFERENCES

AAVSO 1978, Private communication by J. A. Mattei, Director.

Balister, M., Batchelor, R. A., Haynes, R. F., Knowles, S. H., McCulloch, M. G., Robinson, B. J., Wellington, K. J., and Yabsley, D. E. 1977, M.N.R.A.S., 180, 415.

Beckwith, S. V. W. 1978, Private communication.

Brannon, P. J., Church, C. H., and Peters, C. W. 1968, J. Molec. Spectr., 27, 44.

Burdyuzha, V. V., and Varshalovich, D. A. 1973, Soviet Astronomy, 16, 980.

Camy-Peyret, C., Flaud, J. M., Guelachvili, G., and Amiot, C. 1973, Molec. Phys., 26, 825.

Cook, A. H. 1966, Nature, 211, 503.

Destombes, J. L. 1978a, Ph.D. thesis, U. de Lille.

Destombes, J. L. 1978b, Private communication.

Dickinson, D. F., Kollberg, E., and Yngvesson, S. 1975, Ap. J., 199, 131.

Dieke, G. H., and Crosswhite, H. M. 1962, J. Quant. Spectr. Rad. Transfer, 2, 97.

Elitzur, M., Goldreich, P., and Scoville, N. 1976, Ap. J., 205, 384.

Evenson, K. M., Wells, J. S., Radford, H. E. 1970, Phys. Rev. Lett., 25, 199.

Flaud, J. M., and Camy-Peyret, C. 1975, J. Molec. Spectr., 55, 278.

Flaud, J. M., and Camy-Peyret, C. 1978, Private communication.

Geballe, T. R., and Townes, C. H. 1974, Ap. J., 205, 144.

Goldreich, P. 1975, in "Atomic and molecular physics and the interstellar matter," ed. Balian et al. (North-Holland Publishing Company), p. 413.

Goldreich, P., Keeley, D. A., and Kwan, J. Y. 1973, Ap. J., 179, 111.

Goldreich, P., and Scoville, N. 1976, Ap. J., 205, 144.

Harvey, P. M., Bechis, K. P., Wilson, W. J., and Ball, J. A. 1974, Ap. J. Suppl., 27, 331.

Kaifu, N., Buhl, D., and Snyder, L. E. 1975, Ap. J., 195, 359.

Kaplan, S.A., and Pikelner, S.B. 1970, "The Interstellar Medium" (Harvard University Press), p. 231.

Kellermann, K. I., Pauliny-Toth, I. I. K., and Williams, P. J. S. 1969, Ap. J., 157, 1.

Kruszewski, A., Gehrels, T., and Serkowski, K. 1968, A. J., 73, 677.

Lépine, J. R. D. 1978, Private communication.

Lépine, J. R. D., Paes de Barros, M. H., and Gammon, R. H. 1976, Astr. and Ap., 48, 269.

Litvak, M. M. 1969, Ap. J., 156, 471.

Litvak, M. M. 1974, Ann. Rev. Astron. Ap., 12, 97.

Lo, K. Y., Walker, R. C., Burke, B. F., Moran, J. M., Johnston, K. J., and Ewing, M. S. 1975, Ap. J., 202, 650.

London, R., McCray, R., and Chu, S. I. 1977, Ap. J., 217, 442.

Maillard, J. P. 1978, Private communication.

Maillard, J. P., Chauville, J., and Mantz, A. W. 1976, J. Molec. Spectr., 63, 120.

Merrill, P. W. 1960, in "Stellar Atmospheres," ed. J. Greenstein

(Chicago; University of Chicago Press), p. 509.

Mies, F. H. 1974, J. Molec. Spectr., 53, 150.

Milliken, R. C., and White, D. R. 1963, J. Chem. Phys., 39, 3209.

Moran, J. M., Reid, M. J., Lada, C. J., Yen, J. L., Johnston, K. J., and Spencer, J. H. 1978, Ap. J. (Letters), 224, L67.

Morris, D. Radhakrishnan, V., and Seielstad, G. A. 1964, Ap. J., 139, 551.

Palmer, P., and Zuckerman, B. 1967, Ap. J., 143, 727.

Pataki, L., and Kolena, J. 1974, Bull. Am. Astr. Soc., 6, 340.

Reid, M. J. 1976, Ap. J., 207, 784.

Reid, M. J., Muhleman, D. O., Moran, J. M., Johnston, K. J., and Schwartz, P. R. 1977, Ap. J., 214, 60.

Reid, M. J., and Muhleman, D. O. 1978, Ap. J., 220, 229.

Reid, M. J., Moran, J. M., Leach, R. W., Ball, J. A., Johnston, K. J., and Spencer, J. H. 1979, Ap. J. (Letters), 227, L89.

Snyder, L. E., and Buhl, D. 1975, Ap. J., 197, 329.

Spitzer, L. 1978, "Physical Processes in the Interstellar Medium" (John Wiley & Sons, New York).

ter Haar, D., and Pelling, M. A. 1974, Rep. Prog. Phys., 37, 481.

Wallerstein, G. 1973, in "Molecules in the Galactic Environment" ed. Gordon, M. A., and Snyder, L. E. (J. Wiley & Sons, New York).

Wilson, W. J., Barrett, A. H., and Moran, J. M. 1970, Ap. J., 160, 545.

Wilson, W. J., Schwartz, P. R., Neugebauer, G., Harvey, P. M., and Becklin, E. E. 1972, Ap. J., 177, 523.

Wilson, W. J., and Barrett, A. H. 1972, Astr. and Ap., 17, 385.